NextData
Studi Pilota 2° anno
WP 2.6

ISAC-CNR

Elisa Palazzi
Jost von Hardenberg
Luca Filippi
Silvia Terzago
Francesco Toselli (UNITO)
Antonello Provenzale

Incontro Generale NextData, 3-4 Giugno 2014, Roma, CNR-DTA

1. *Analysis of* ***water resources in the Himalaya-Karakoram*** *and* ***interaction between monsoon and mid-latitude perturbations (D2.6.2a)***

2. *Estimation of the changes in the hydrological cycle,* ***snow cover and water availability in high altitude areas (HKKH, Alps) (D2.6.2c)***

3. *Simulations of the last 150 years climate with an Earth system models of intermediate complexity (****PlaSIM****) and preparation of paleoclimate simulations* ***(D2.6.2e)***

1. Analysis of water resources in the Himalaya-Karakoram and interaction between monsoon and mid-latitude perturbations

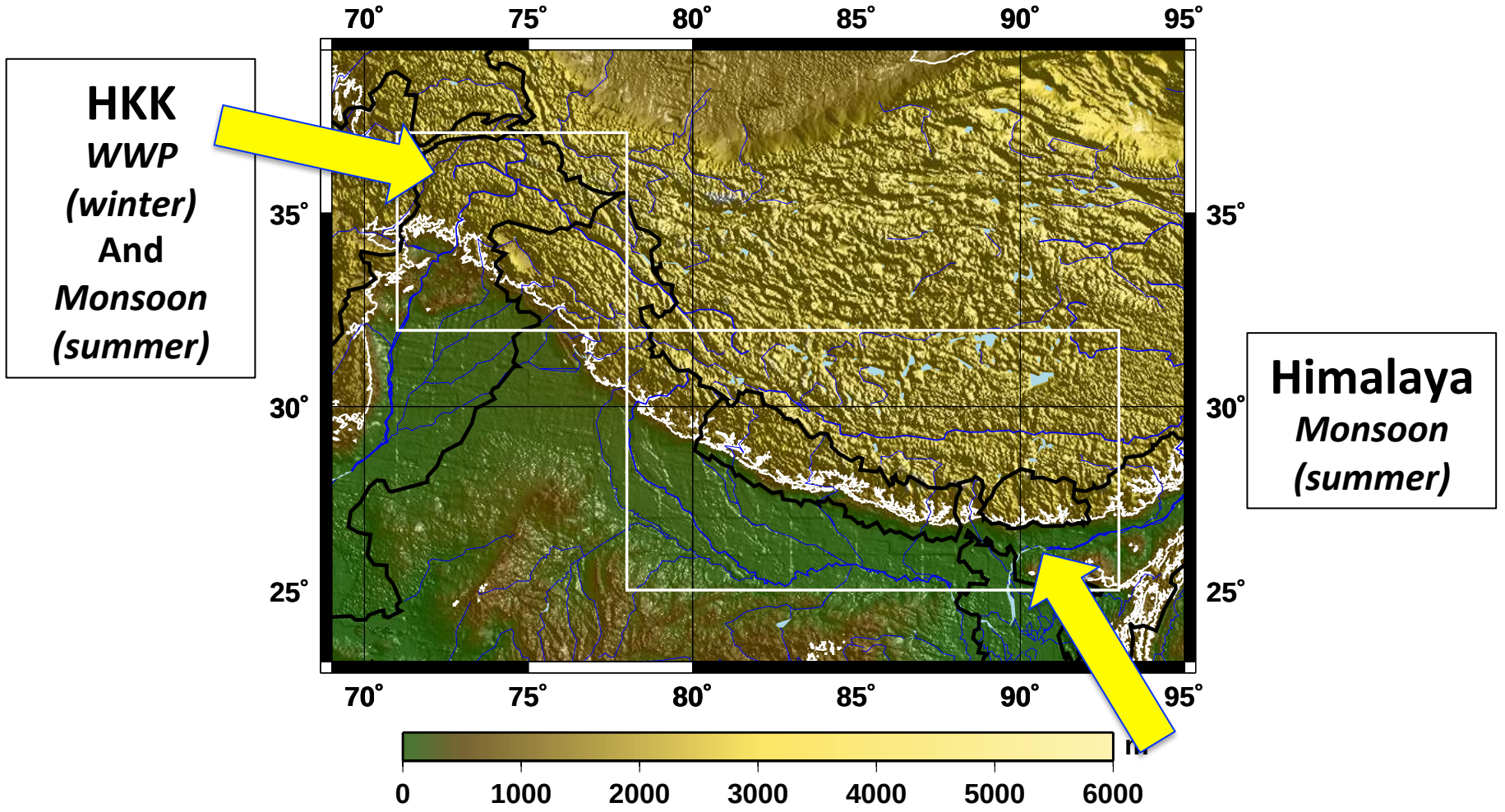

Palazzi, von Hardenberg, Provenzale, JGR 2013

Present and future precipitation climatology in HKK and Himalaya

- Annual cycle climatology
- Long-term trends
- Precipitation changes

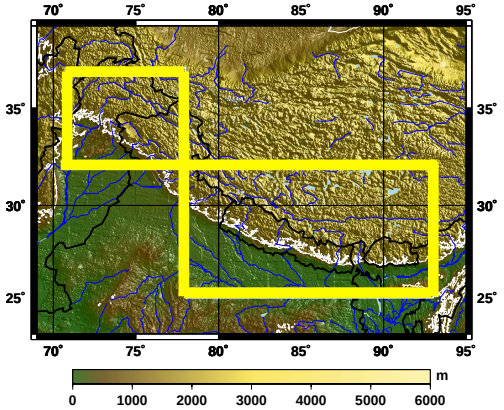

Precipitation in HKK and teleconnections

Multi-decadal variations in the relationship between NAO and winter precipitation in the Karakoram

- ***Observational data*** *(gridded precipitation datasets): station-based; satellite; merged (es. GPCP)*
- ***Reanalyses***
- ***GCMs****: EC-Earth + CMIP5 ensemble*

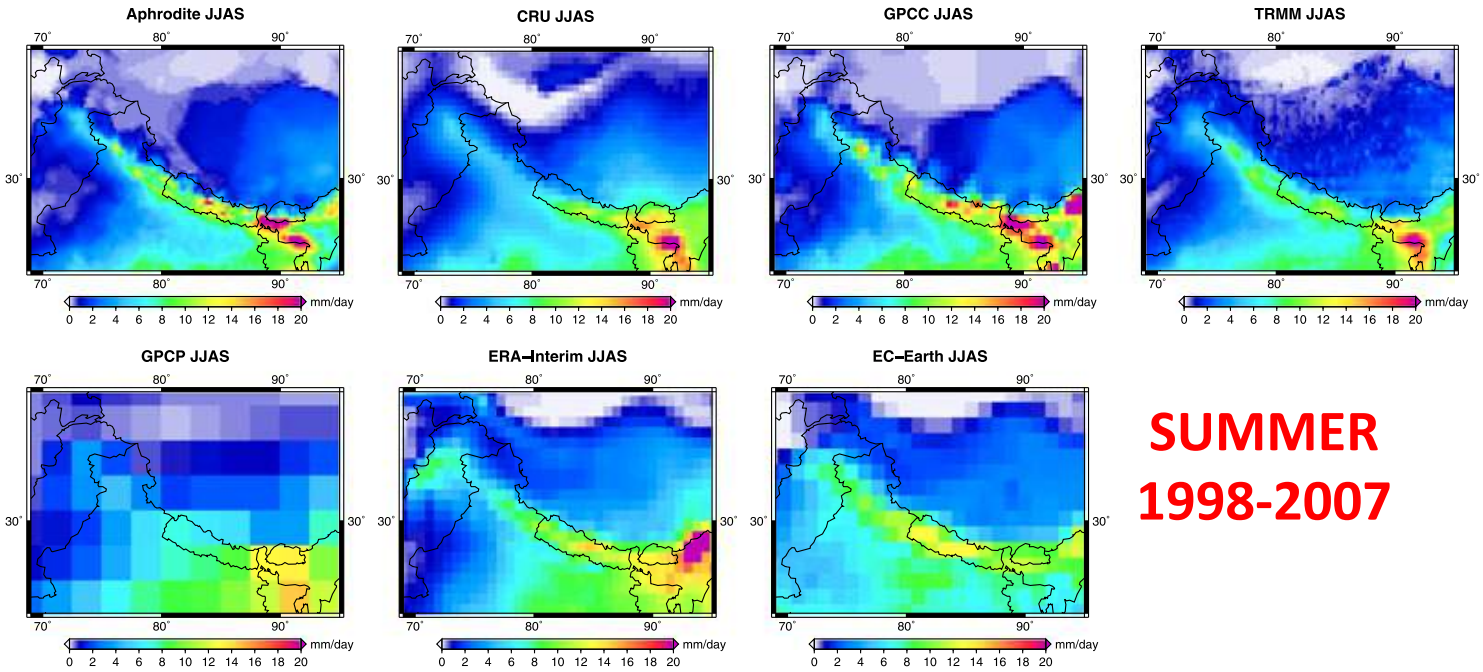

Aphrodite
CRU
GPCC
TRMM

SUMMER
1998-2007

GPCP
ERA-Interim
EC-Earth

Figure 2. Multiannual mean (1998–2007) of summer (JJAS) precipitation over the region between 69°E–95°E and 23°N–39°N from the APHRODITE, CRU, GPCC, TRMM, GPCP, ERA-Interim, and EC-Earth model data sets.

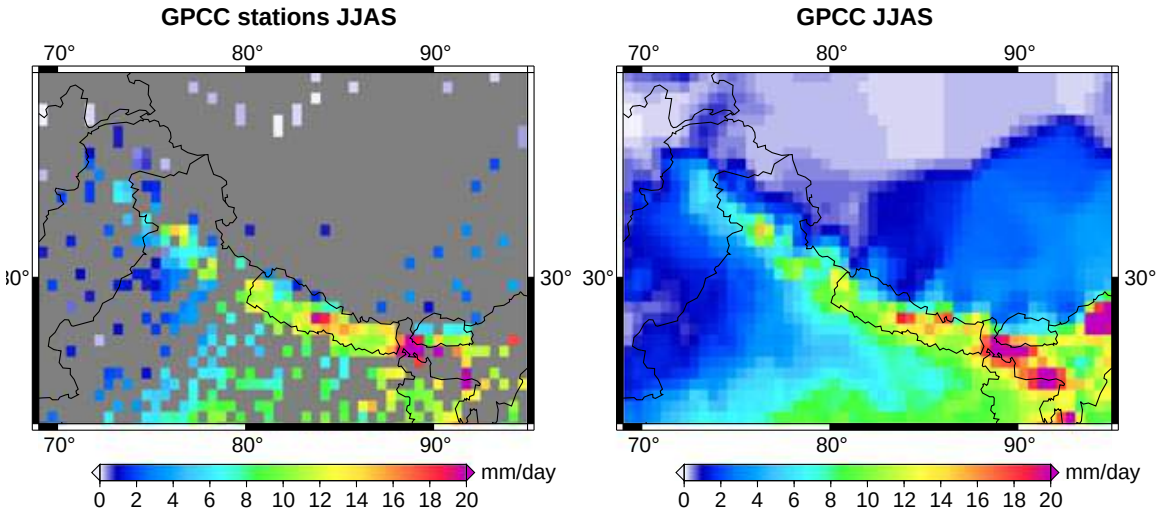

Sparse station coverage
→ interpolation
→ uncertainty in the gridded product

Palazzi, von Hardenberg, Provenzale, JGR 2013

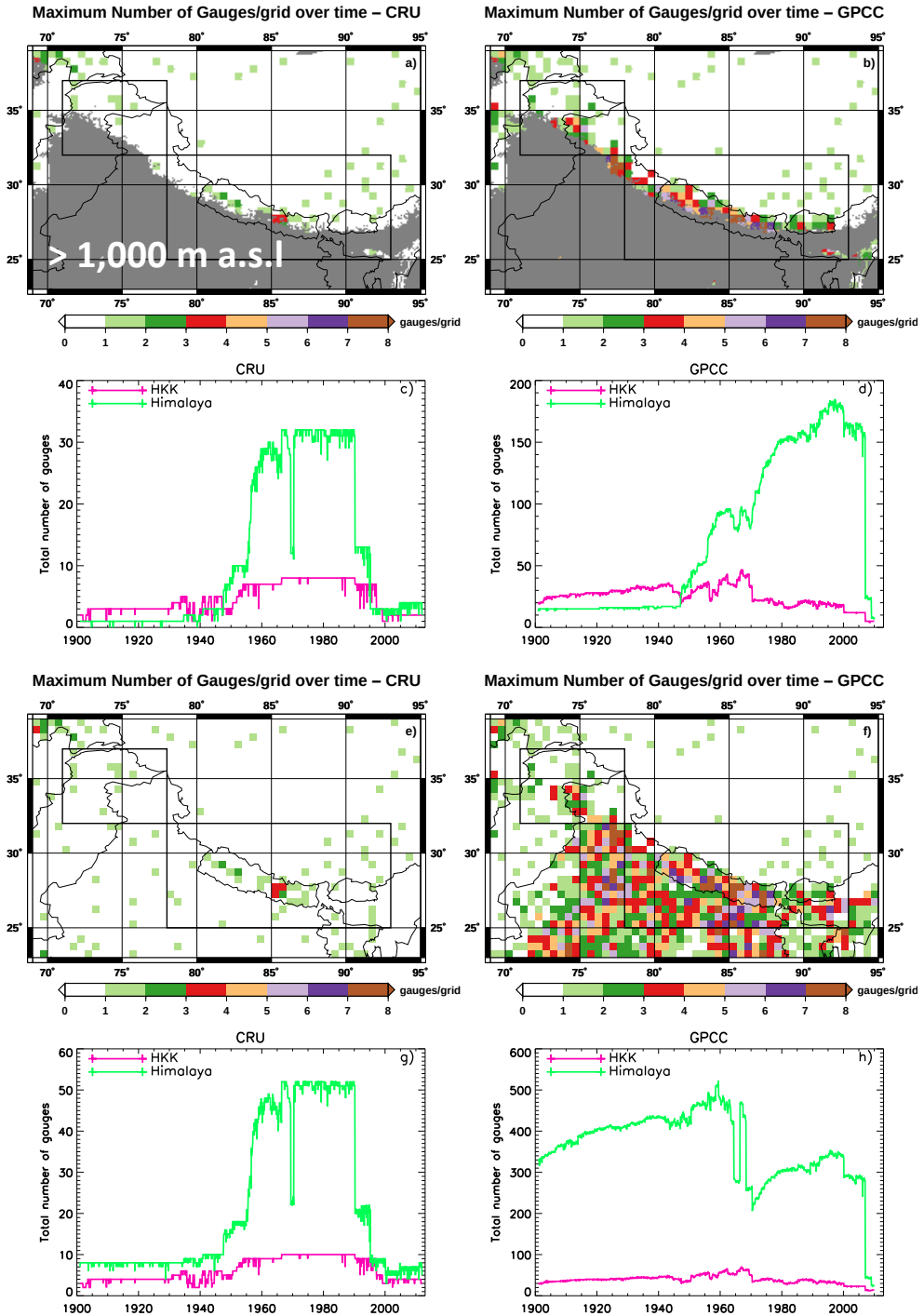

Maximum number of stations per pixel in the period 1901-2012 (CRU) and 1901-2010 (GPCC)

Time series of the number of stations per pixels for CRU (left) and GPCC (right) in the HKK and Himalaya regions

Palazzi, von Hardenberg, Terzago and Provenzale, under revision, Clim Dyn

Annual cycle Climatology

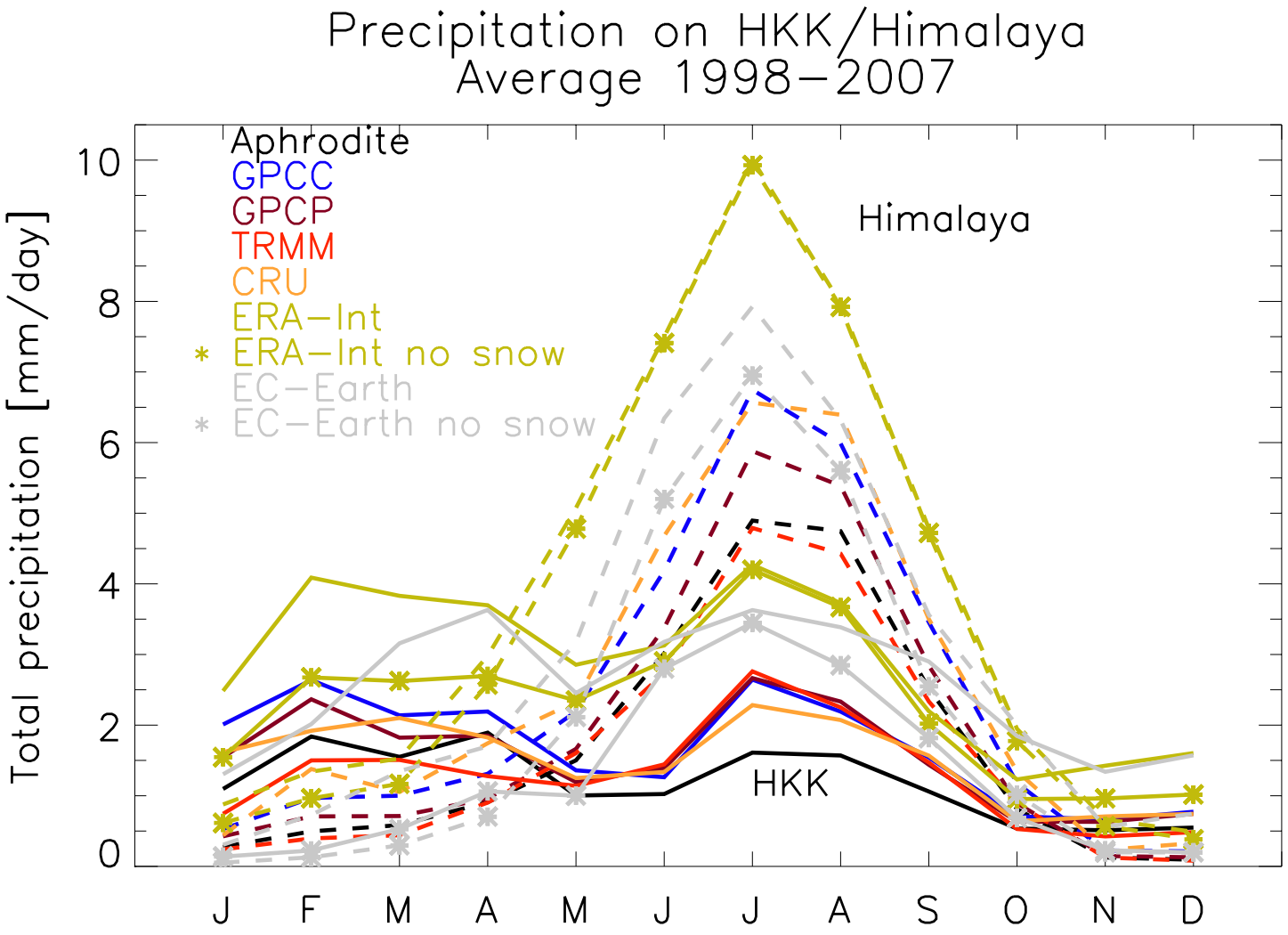

Palazzi, von Hardenberg, Provenzale, JGR 2013

Annual cycle Climatology

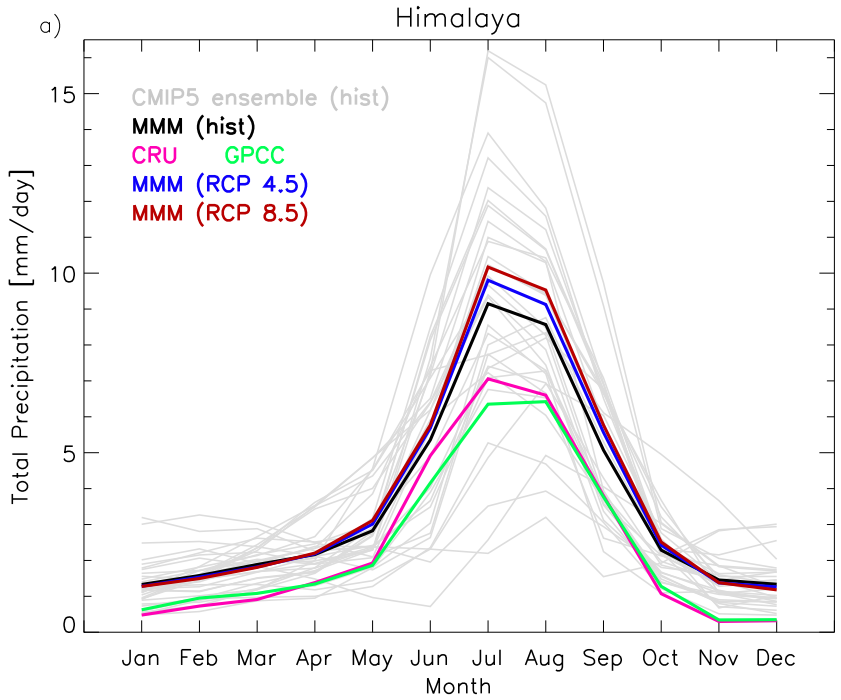

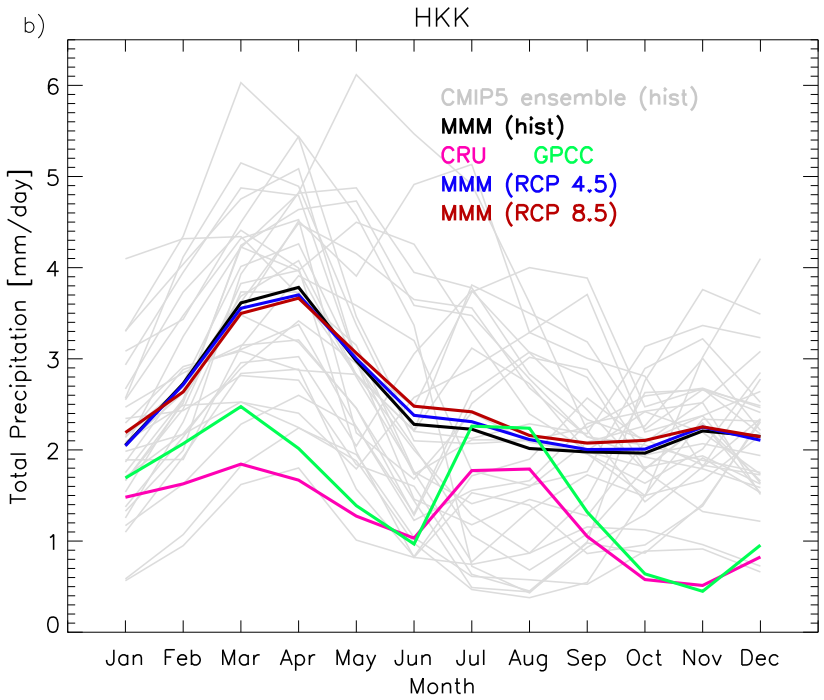

Inter-model SPREAD

	(a) Jan	(b) Feb	(c) Mar	(d) Apr	(e) May	(f) Jun	(g) Jul	(h) Aug	(i) Sep	(l) Oct	(m) Nov	(n) Dec
Historical												
Himalaya	49	39	30	34	38	43	37	32	39	36	47	47
HKK	38	32	27	26	38	53	59	53	43	30	30	35
RCP 4.5												
Himalaya	51	40	30	37	39	42	37	31	39	35	50	56
HKK	36	32	30	30	39	53	58	53	42	33	32	34
RCP 8.5												
Himalaya	51	39	29	39	40	41	37	31	37	37	48	55
HKK	36	30	29	31	40	52	57	52	44	33	29	35

Palazzi, von Hardenberg, Terzago and Provenzale, under revision, Clim Dyn

Himalaya

HKK

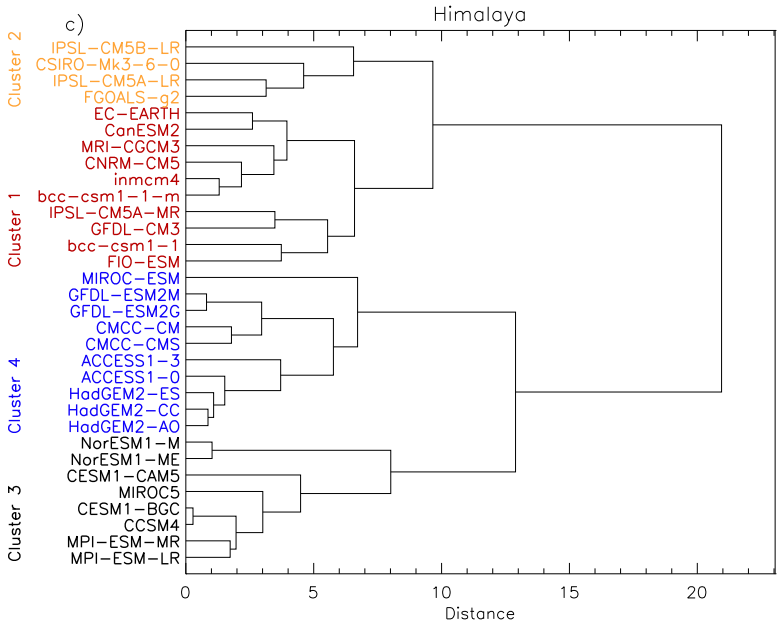

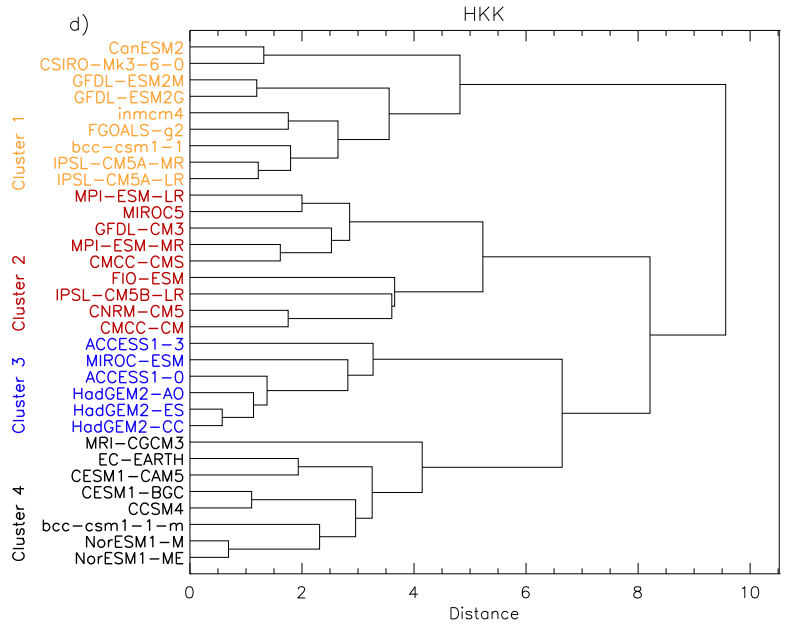

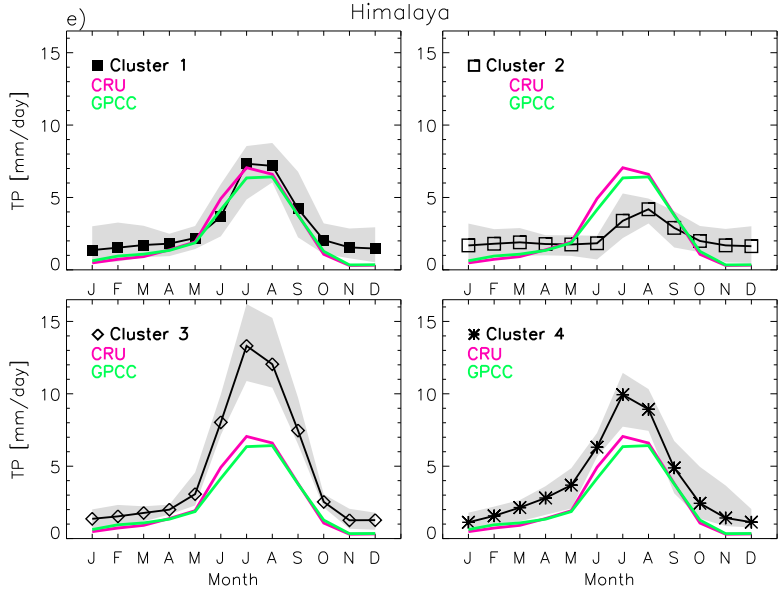

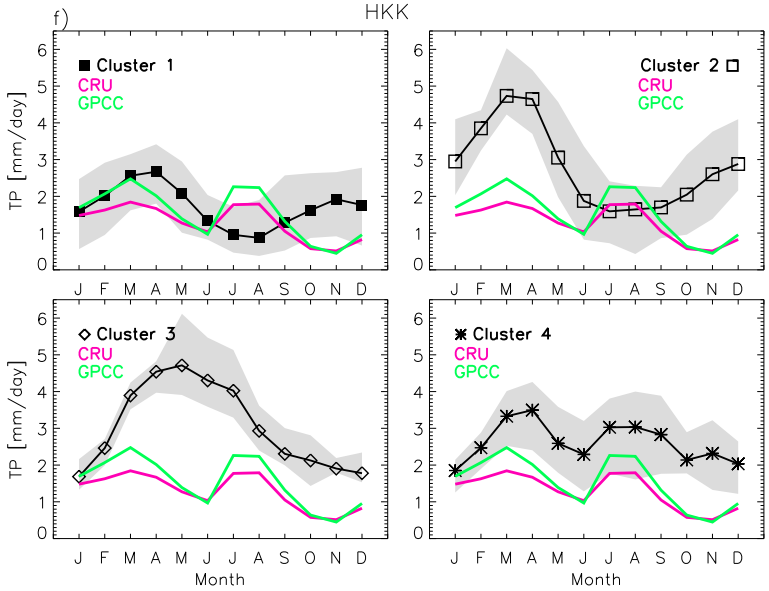

Palazzi, von Hardenberg, Terzago and Provenzale, under revision, Clim Dyn

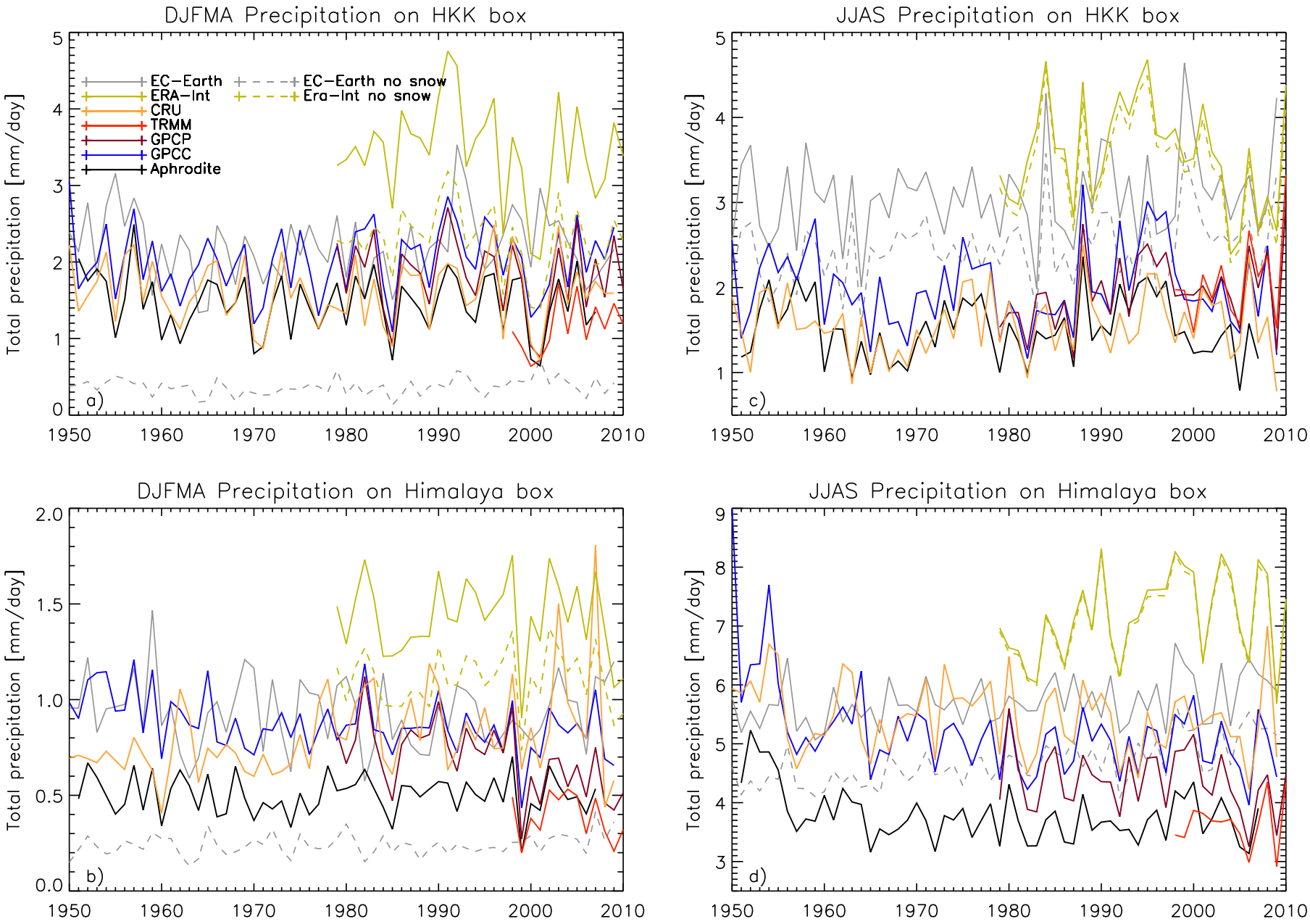

Palazzi, von Hardenberg, Provenzale, JGR 2013

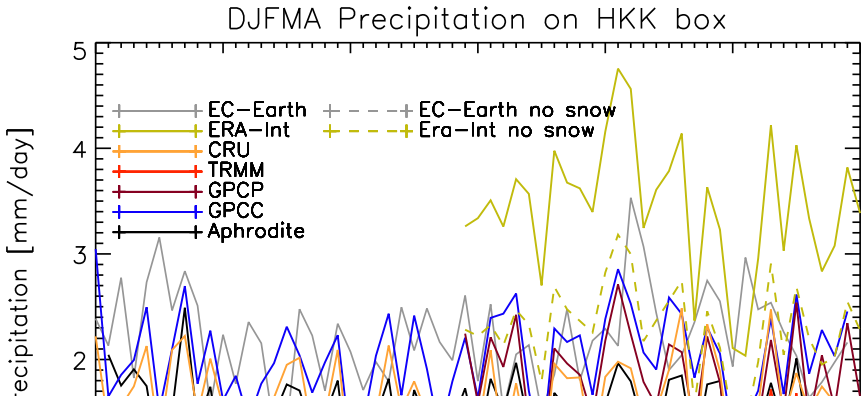

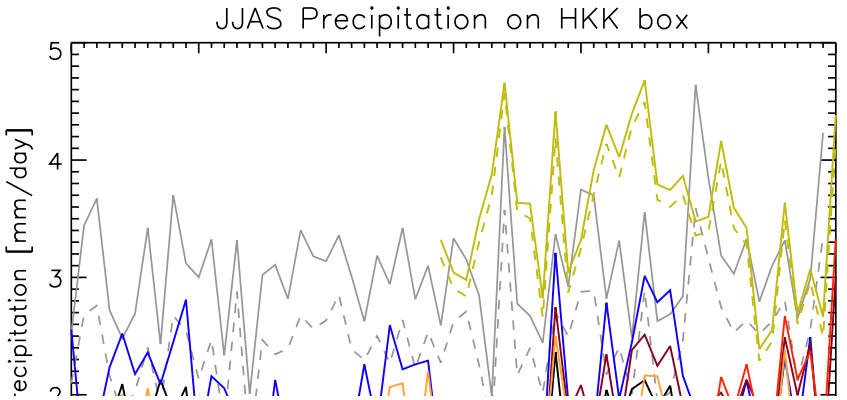

Table 4. Precipitation Trends (in mm d^{-1} yr^{-1}) in the HKK and Himalaya During Summer (JJAS) and Winter (DJFMA) for the Various Data Sets (in Parentheses the Years Over Which Trends Have Been Calculated). Bold Figures are Significant at the 95% Level (*p*-value Indicated in Brackets)

	JJAS		DJFMA	
	Himalaya	HKK	Himalaya	HKK
APHRODITE (1951–2007)	**–0.010(*p*=0.001)**	0.0	0.0	–0.003
CRU (1950–2009)	–0.008	0.002	**0.005(*p*=0.004)**	–0.001
GPCC (1950–2009)	**–0.021(*p*=0.001)**	0.0	**–0.004(*p*=0.000)**	0.002
TRMM (1998–2010)	0.015	0.057	–0.006	0.041
GPCP (1979–2010)	–0.012	**0.017(*p*=0.045)**	**–0.010(*p*=0.001)**	–0.007
ERA-Interim (1979–2010)	0.027	–0.011	–0.002	–0.012
EC-Earth (1950–2009)	**0.008(*p*=0.002)**	0.005	–0.001	0.0
* ERA-Interim (1979–2010)	0.027	–0.011	0.0	–0.007
* EC-Earth (1950–2009)	**0.014(*p*=0.000)**	**0.007(*p*=0.027)**	**0.001(*p*=0.050)**	0.001

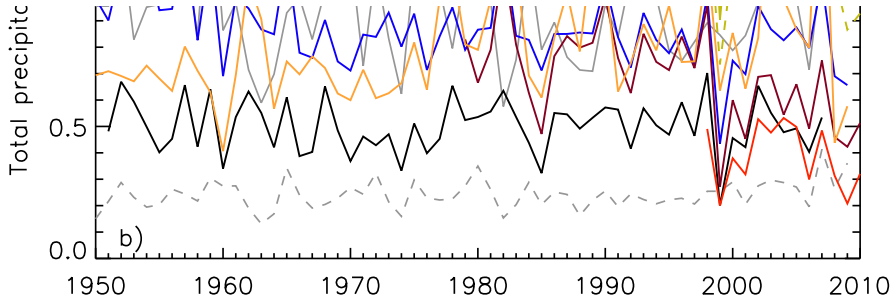

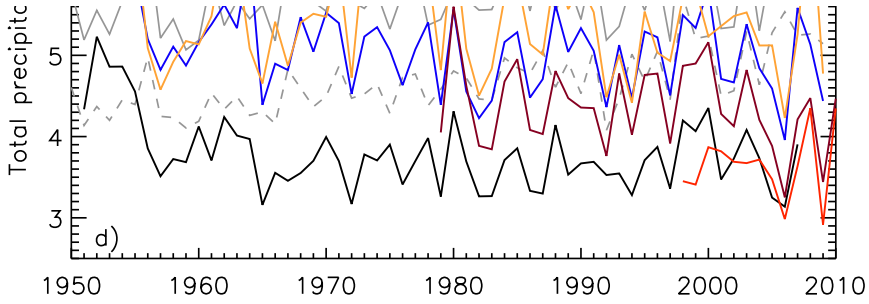

Palazzi, von Hardenberg, Provenzale, JGR 2013

Himalaya

	JJAS			DJFMA		
	Historical 1901-2005	RCP4.5 2006-2100	RCP8.5 2006-2100	Historical 1901-2005	RCP4.5 2006-2100	RCP8.5 2006-2100
Observations						
CRU	**-0.416**			0.033		
GPCC	**-1.445**			**-0.355**		
CMIP5 models						
bcc-csm1-1-m	0.010	0.171	**0.827**	0.170	-0.131	-0.066
bcc-csm1-1	0.026	0.847	**2.076**	-0.015	0.391	**0.797**
CCSM4	0.283	0.507	**1.746**	-0.123	-0.084	-0.127
CESM1-BGC	-0.114	**0.837**	**1.866**	-0.042	-0.088	-0.193
*CESM1-CAM5	-0.395	**2.588**	**3.806**	0.020	0.033	0.135
EC-Earth	**0.516**	0.003	**1.082**	0.101	**0.162**	0.097
FIO-ESM	0.042	**-1.547**	-0.828	0.000	-0.099	-0.328
GFDL-ESM2G	0.164	**0.711**	**4.198**	0.101	-0.040	0.242
GFDL-ESM2M	-0.014	**1.445**	**2.534**	0.127	0.140	**0.299**
MPI-ESM-LR	-0.114	-0.356	0.183	-0.082	-0.188	-0.233
MPI-ESM-MR	0.464	0.153	-0.011	-0.262	-0.044	**-0.483**
***CanESM2**	**-1.009**	**1.553**	**2.214**	0.003	-0.012	**0.331**
CMCC-CMS	0.136	0.610	-0.035	0.047	**-0.484**	**-0.460**
CNRM-CM5	0.194	0.567	**1.769**	0.034	0.238	**0.462**
***CSIRO-Mk3-6-0**	-0.079	0.162	**0.785**	-0.084	**0.165**	0.129
***GFDL-CM3**	**-0.799**	**4.873**	**6.583**	0.134	0.022	-0.182
INM-CM4	0.073	**0.758**	**1.874**	-0.036	0.054	**-0.238**
IPSL-CM5A-LR	-0.088	**0.860**	**1.021**	-0.215	0.135	**-0.641**
IPSL-CM5A-MR	0.039	**1.498**	**2.603**	-0.031	0.069	-0.310
IPSL-CM5B-LR	-0.133	**1.042**	**1.602**	-0.012	0.172	0.315
***MRI-CGCM3**	0.031	-0.265	0.330	-0.123	-0.022	0.215
CMCC-CM	-0.161	0.239	**0.956**	0.161	-0.212	**-0.524**
FGOALS-g2	**0.313**	**0.914**	**2.215**	0.190	**-0.261**	**-0.351**
***HadGEM2-AO**	**-0.436**	**1.228**	**1.129**	**-0.150**	0.061	-0.051
***ACCESS1-0**	**-0.476**	**0.699**	**1.150**	-0.105	-0.063	**-0.183**
***ACCESS1-3**	**-0.537**	**1.953**	**2.996**	0.076	-0.017	-0.071
***HadGEM2-CC**	**-0.746**	**1.662**	**1.507**	-0.086	**0.227**	-0.076
***HadGEM2-ES**	**-0.445**	**1.356**	**1.295**	**-0.189**	0.012	-0.091
***MIROC5**	**0.585**	**2.210**	**3.769**	-0.064	0.062	**0.292**
***MIROC-ESM**	0.358	**1.620**	**2.432**	-0.239	0.266	-0.036
***NorESM1-M**	-0.045	**1.838**	**2.469**	0.103	0.053	-0.110
***NorESM1-ME**	-0.075	**1.976**	**2.295**	0.230	-0.017	-0.182
MMM	-0.076	**1.027**	**1.860**	-0.011	0.016	-0.051
Multi-Model Median	**-0.205**	**1.254**	**1.317**	-0.034	-0.070	**-0.093**
Cluster 1 MMM	-0.068	**0.500**	**1.357**	-0.021	0.071	-0.025
Cluster 1 Multi-Model Median	-0.047	**0.471**	**1.408**	-0.031	0.060	-0.139

HKK

	JJAS			DJFMA		
	Historical 1901-2005	RCP4.5 2006-2100	RCP8.5 2006-2100	Historical 1901-2005	RCP4.5 2006-2100	RCP8.5 2006-2100
Observations						
CRU	0.097			**0.332**		
GPCC	0.101			0.002		
CMIP5 models						
bcc-csm1-1-m	**0.544**	0.596	0.493	-0.091	0.126	-0.078
bcc-csm1-1	-0.061	0.158	0.054	-0.238	-0.198	0.011
CCSM4	-0.019	0.004	0.255	-0.264	-0.089	-0.292
CESM1-BGC	-0.352	0.522	-0.193	-0.271	-0.117	-0.529
*CESM1-CAM5	**0.550**	**-0.739**	0.054	-0.045	-0.058	0.226
EC-Earth	0.186	0.023	0.033	-0.013	**0.458**	0.344
FIO-ESM	0.335	0.116	0.184	-0.228	-0.506	**-1.141**
GFDL-ESM2G	-0.003	0.297	**0.674**	0.159	-0.070	0.025
GFDL-ESM2M	**0.628**	0.254	**0.613**	0.017	-0.126	0.044
MPI-ESM-LR	-0.013	-0.064	-0.258	-0.510	-0.528	**-1.140**
MPI-ESM-MR	-0.052	0.173	0.005	-0.286	0.199	**-1.010**
***CanESM2**	0.030	-0.104	0.011	0.000	-0.114	0.181
CMCC-CMS	0.261	-0.013	-0.129	-0.194	**-0.871**	**-0.840**
CNRM-CM5	0.040	-0.102	**0.338**	0.339	0.160	**0.989**
***CSIRO-Mk3-6-0**	0.079	0.143	-0.054	-0.242	**0.378**	**0.554**
***GFDL-CM3**	-0.071	**0.334**	0.296	0.039	-0.066	-0.398
INM-CM4	0.044	0.052	0.196	-0.178	-0.098	**-0.591**
IPSL-CM5A-LR	-0.009	**-0.287**	-0.120	-0.250	0.426	-0.600
IPSL-CM5A-MR	0.188	0.065	**0.300**	-0.373	0.469	-0.234
IPSL-CM5B-LR	-0.015	0.151	**0.633**	-0.106	0.476	**0.736**
***MRI-CGCM3**	**0.462**	-0.214	**0.470**	0.014	0.275	**1.117**
CMCC-CM	0.147	-0.045	0.073	-0.163	0.332	0.305
FGOALS-g2	0.055	**-0.204**	0.192	0.185	**-0.578**	**-0.608**
***HadGEM2-AO**	0.003	0.206	0.044	-0.128	0.254	**0.418**
***ACCESS1-0**	-0.133	**-0.423**	-0.196	0.181	0.013	0.167
***ACCESS1-3**	0.062	**-0.276**	-0.351	0.142	0.085	**0.300**
***HadGEM2-CC**	-0.243	0.189	0.142	-0.099	**0.345**	0.187
***HadGEM2-ES**	-0.206	**0.271**	0.265	-0.046	-0.009	0.242
***MIROC5**	**0.300**	0.238	**1.100**	-0.037	-0.017	-0.248
***MIROC-ESM**	-0.160	-0.216	0.002	0.019	-0.166	**-0.598**
***NorESM1-M**	-0.115	0.290	0.412	0.023	-0.131	-0.105
***NorESM1-ME**	**0.534**	0.281	0.425	0.308	**-0.452**	**-0.530**
MMM	**0.094**	0.054	**0.186**	**-0.073**	-0.006	**-0.097**
Multi-Model Median	0.117	0.116	**0.170**	-0.071	-0.063	**-0.157**
Cluster 4 MMM	0.068	0.002	0.116	-0.163	-0.025	**-0.327**
Cluster 4 Multi-Model Median	0.174	-0.194	-0.220	-0.134	-0.007	**-0.362**

CMIP5 models

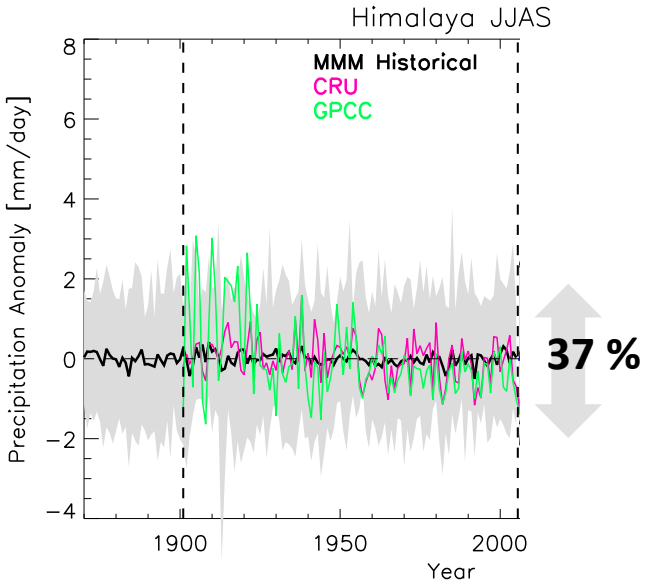

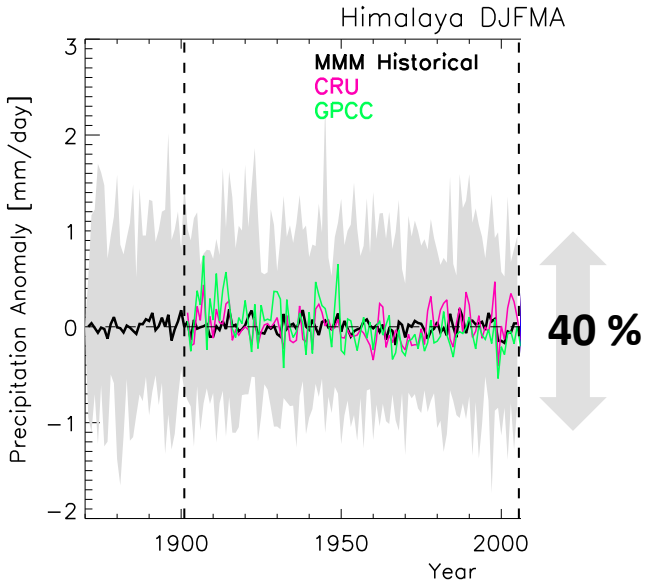

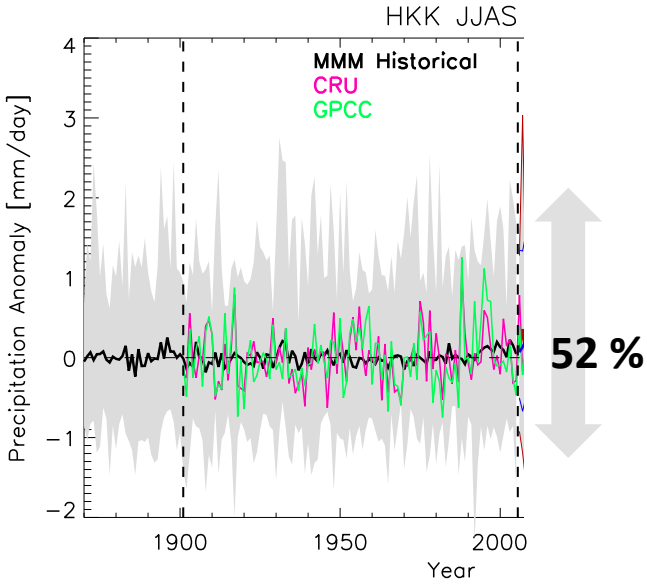

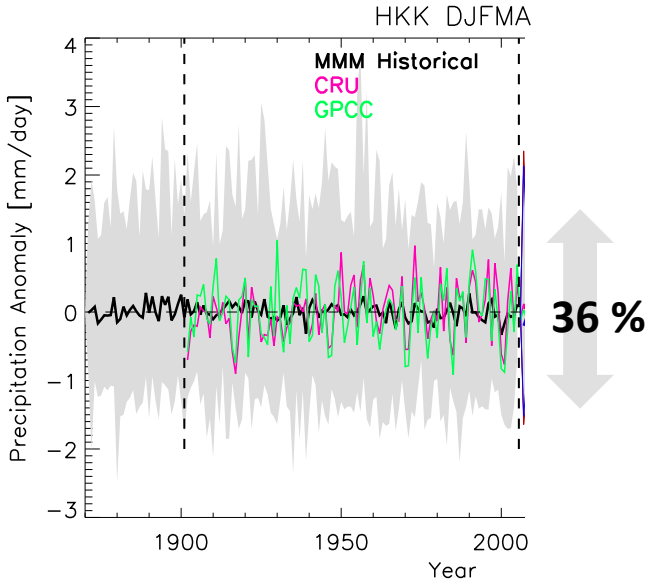

Palazzi, von Hardenberg, Terzago and Provenzale, under revision, Clim Dyn

CMIP5 models

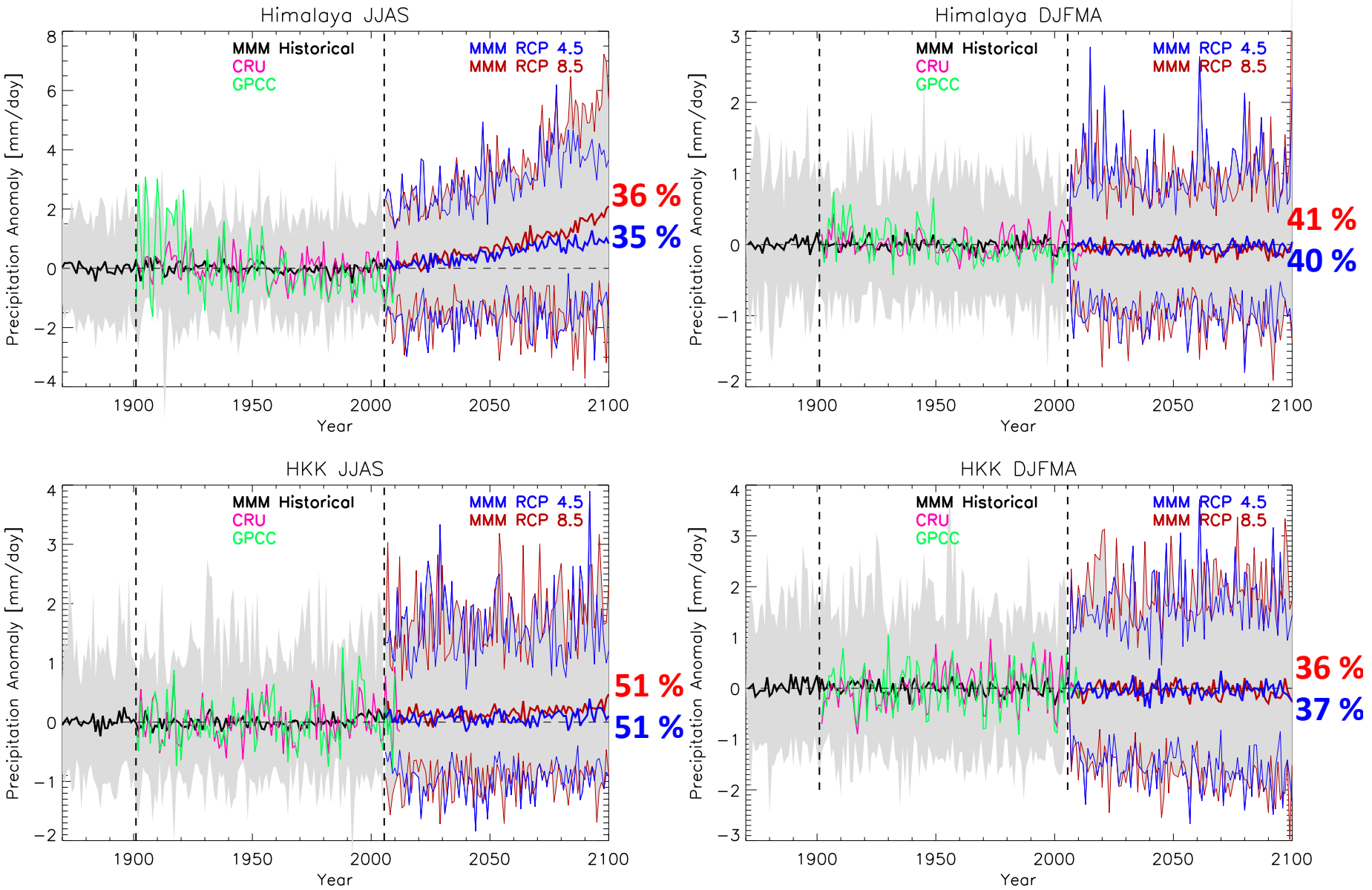

Palazzi, von Hardenberg, Terzago and Provenzale, under revision, Clim Dyn

Multi-decadal variations in the relationship between NAO and winter precipitation in the Karakoram

- Winter precipitation over the HKK and western Himalayas is generated by Western Weather Patterns, whose dynamics is affected by the NAO
- Evidence of the correlation between NAO and winter precipitation in the HKK in the observations/reanalyses
- Analysis of the mechanisms underlying the relationship and secular variations of the NAO-precipitation relationship in the last century

- *Gridded precipitation datasets*
- *ERA40 and 20CR reanalyses*

Filippi, Palazzi, von Hardenberg, and Provenzale, under review, J. Clim

NAO-HKK precipitation correlation: observational evidence

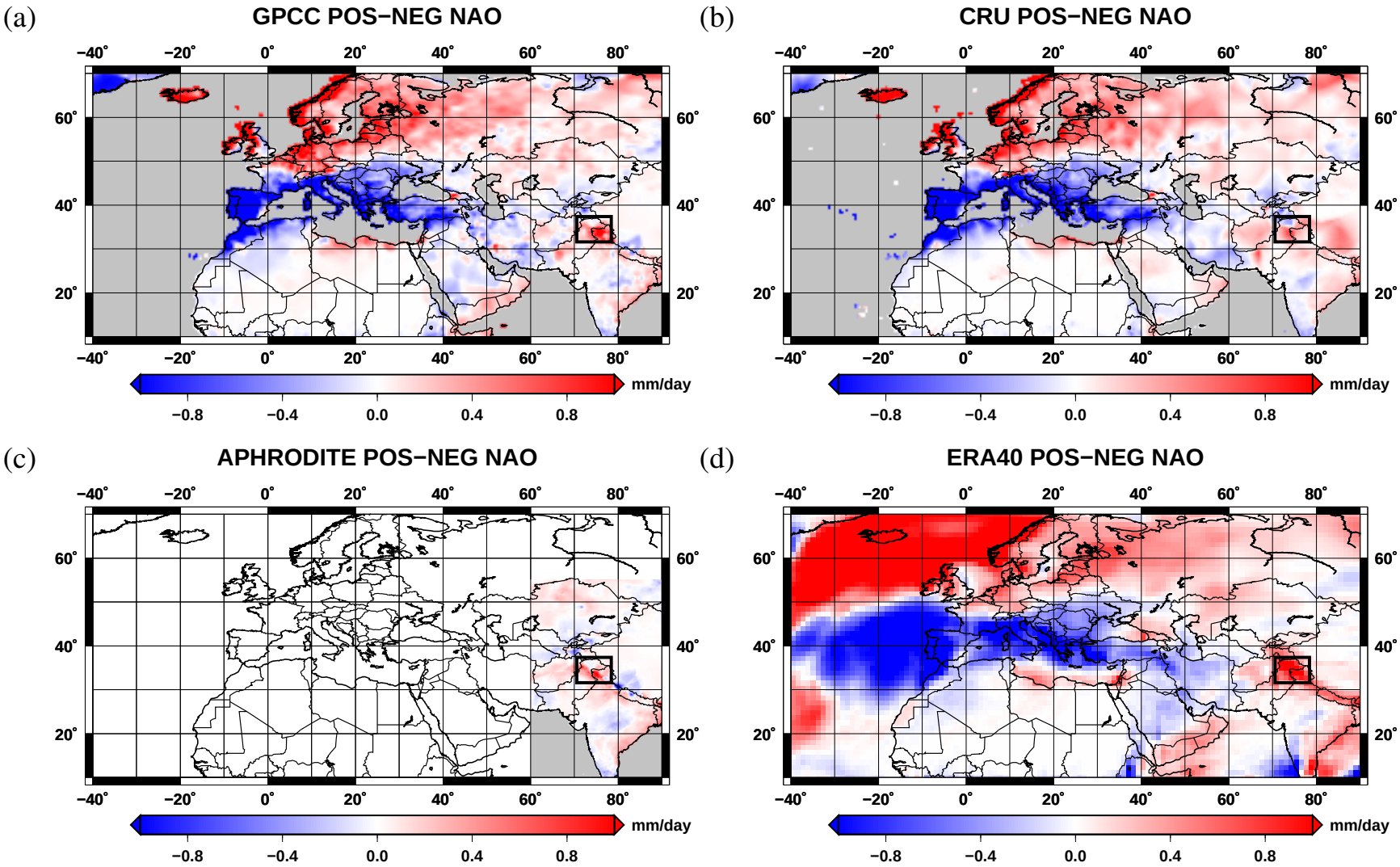

Larger precipitation is typically recorded during positive NAO

Filippi, Palazzi, von Hardenberg, and Provenzale, under review, J. Clim

NAO-HKK precipitation correlation: Mechanism

The NAO **regulates the intensity of westerly winds in the region of the Middle East jet stream**, from North Africa to southeastern Asia.
Positive NAO phase → westerlies over this area are intensified from the upper-tropospheric jet to the lower levels. The strengthening of the jet intensifies the WWPs, while the anomaly in the middle-lower troposphere produces a faster transport of humidity towards the HKK

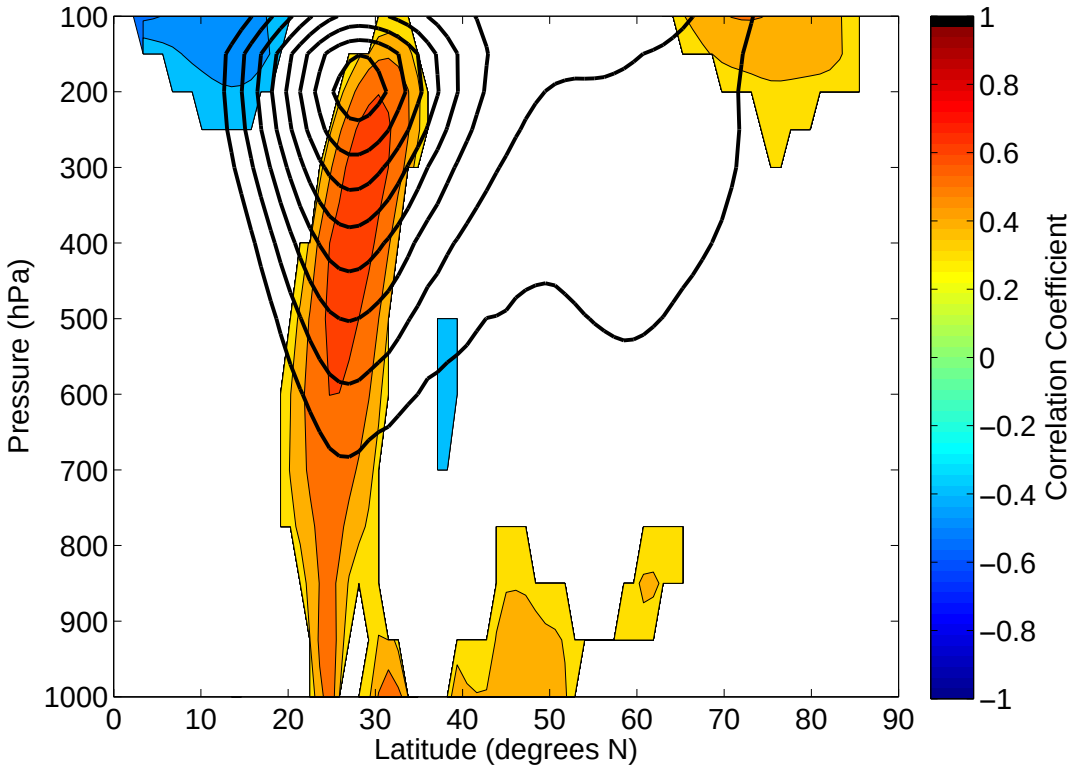

Filled contours: correlation coefficients (95% confidence level) between the NAO and winter zonal wind (40-70°E average)

Black contours: climatology of winter zonal wind (40-70°E average) → position of the MEJS

Filippi, Palazzi, von Hardenberg, and Provenzale, under review, J. Clim

NAO-HKK precipitation correlation: Mechanism

(a)

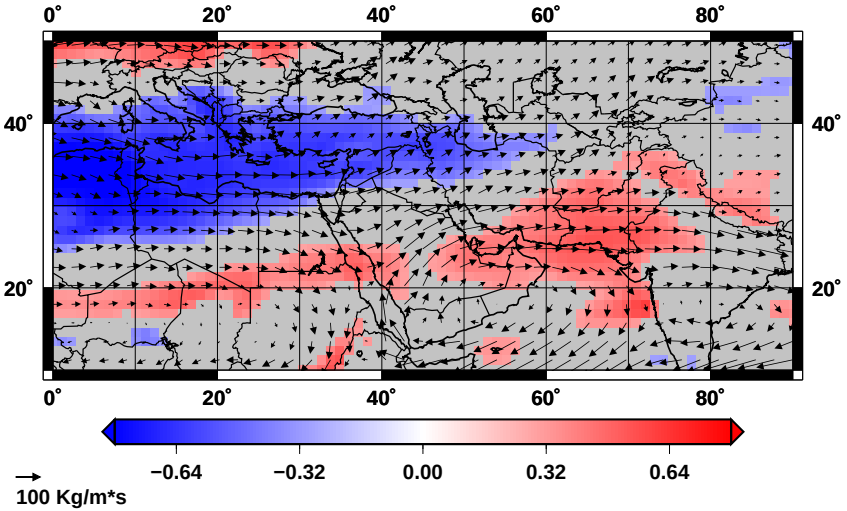

(b)

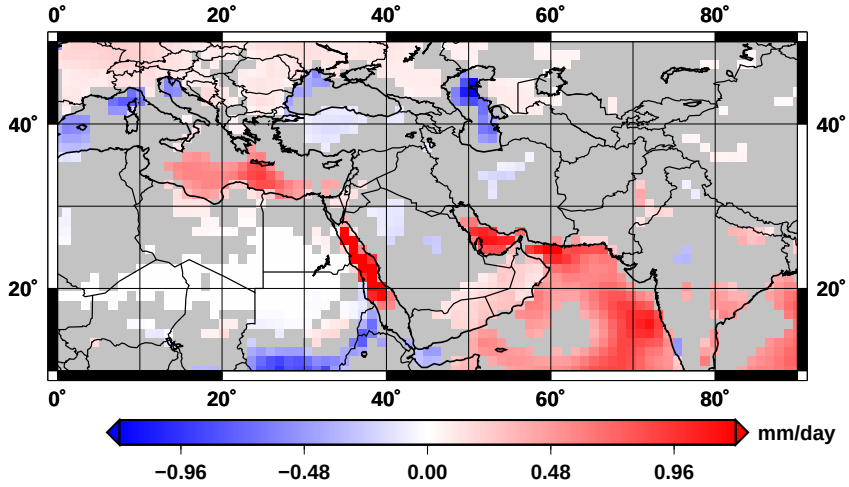

(c)

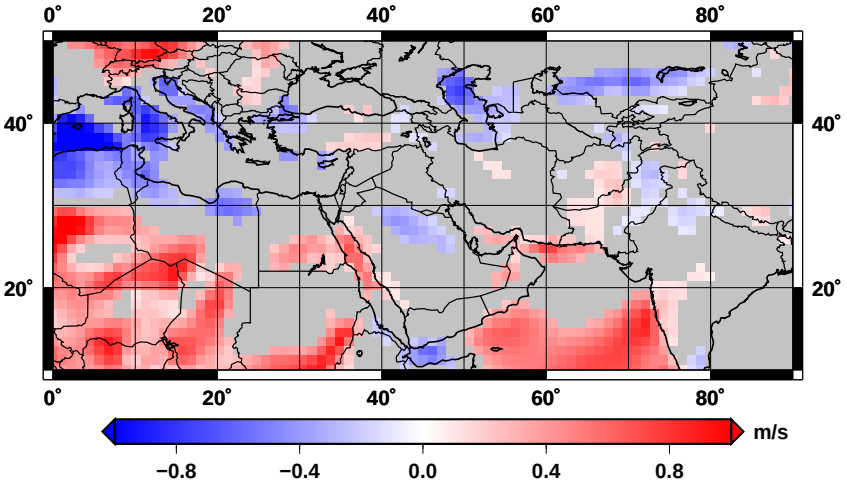

- **The intensity of moisture transport from source regions to the HKK is significantly larger during the positive NAO phase, sustaining wetter than normal conditions in winter in the HKK.**

- **During positive NAO phases, enhanced evaporation from the Persian Gulf, northern Arabian Sea and Red Sea occurs, due to higher surface wind speed.**

NAO-HKK precipitation correlation: Secular variations

Sliding correlations over 21-year moving windows between the NAOI and the time series of precipitation averaged in the HKK domain from GPCC, CRU, APHRODITE and ERA40.

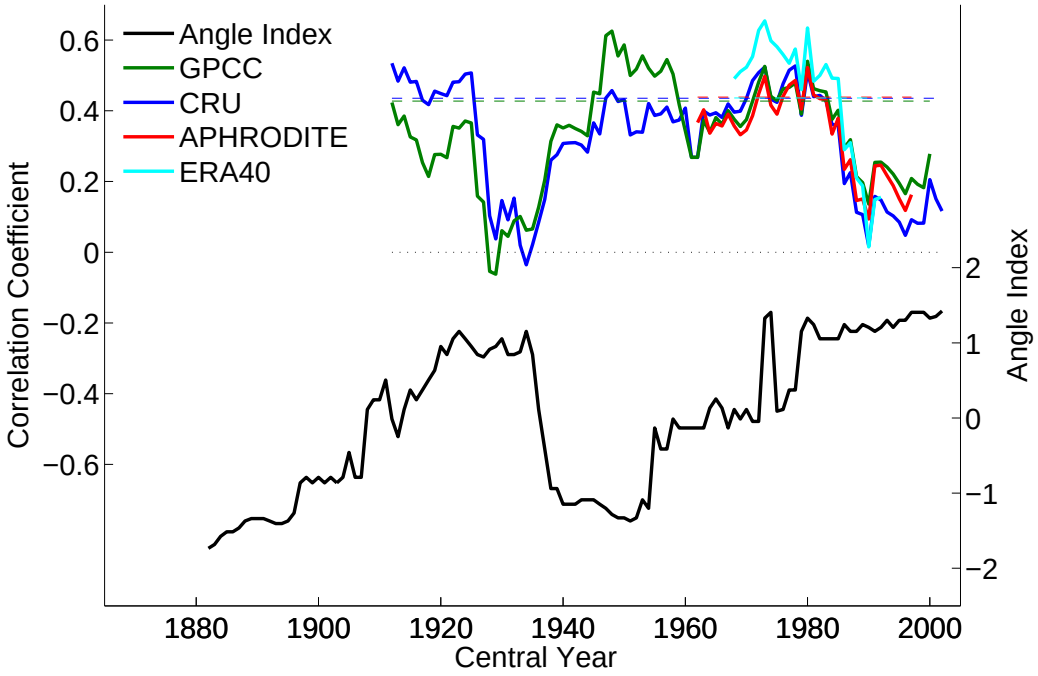

Precipitation datasets covering the 20th century show an **alternation of periods of strong and weaker influence of the NAO on precipitation in the HKK.**

These variations are associated with changes in the spatial pattern of the NAO (antiphase): the relative position of the two centers of action of the NAO determines to what extent it can modulate the MEJS, affecting precipitation in the HKK.

2. Estimation of the changes in the hydrological cycle, snow cover and water availability in high altitude areas

- ✓ Snowpack changes in the Hindu-Kush Karakoram Himalaya from CMIP5 Global Climate Models

*- Global Monthly EASE-Grid **Snow Water Equivalent** Climatology (NSIDC)*
*- AMSR-E/Aqua Monthly L3 Global **Snow Water Equivalent** (level-3) monthly data (NASA EOS Aqua satellite)*
*- Daily **Snow Depth** Analysis Data by the Canadian Meteorological Centre (CMC)*
*- ERA-Interim/Land reanalysis (**SND, SWE**)*
*- Climate Forecast System Reanalysis (CFSR, NCEP) (**SND, SWE**)*
*- 20th Century Reanalysis version 2 (20CRv2) (**SND, SWE**)*
*- CMIP5 GCMs (**SND → 28/35, SWE → 18/35**)*

- ✓ Improvement of snow models and sensitivity to meteorological forcing (ongoing and perspective)

Terzago, von Hardenberg, Palazzi and Provenzale, under 2nd review, JHM

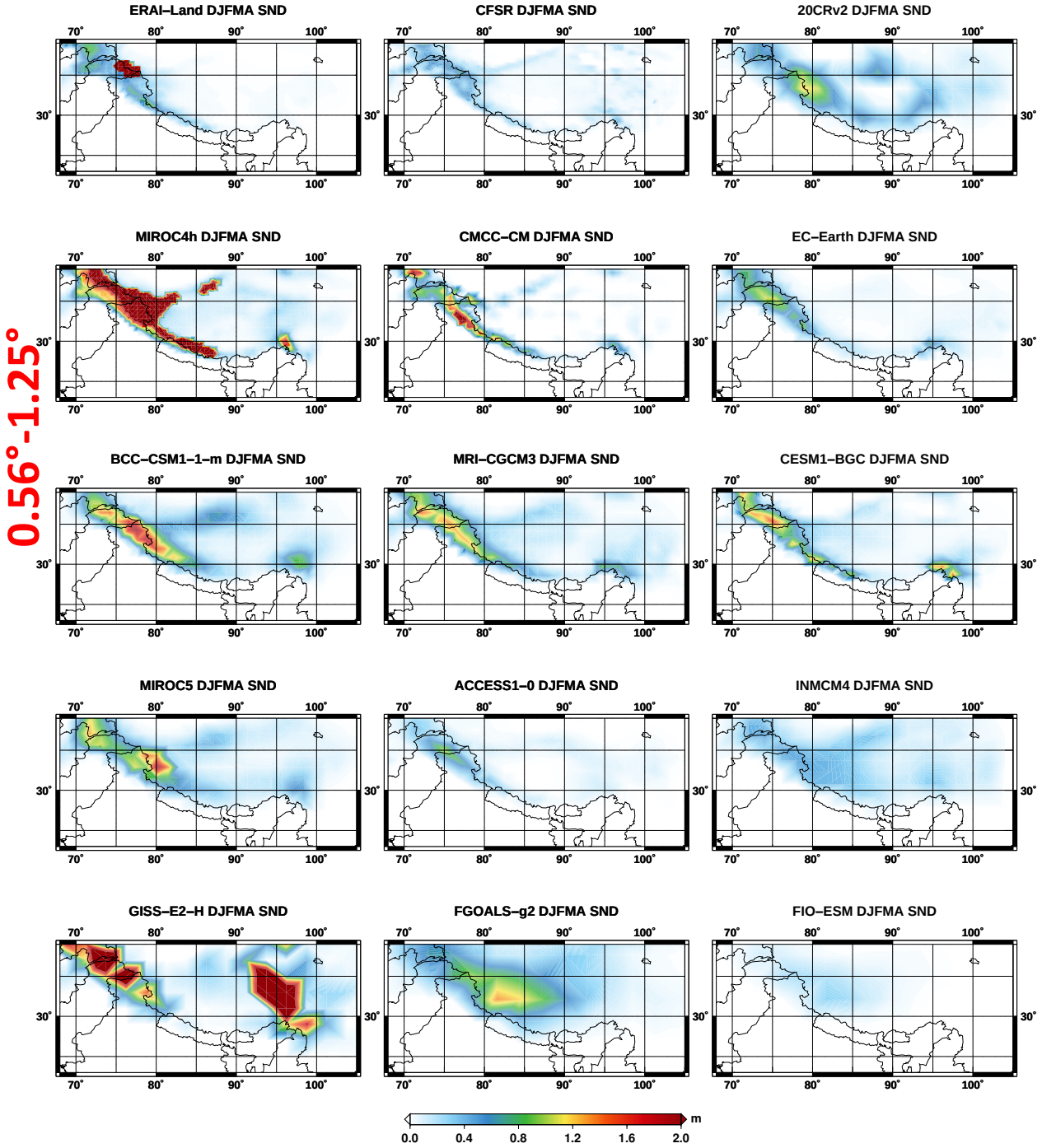

0.56°-1.25°

High-resolution GCMs. They depict similar spatial patterns with snow depth peaking over the HKK and decreasing towards the Himalya and TP

Several low spatial resolution models tend to represent either a very thick or very shallow snowpack in winter, or a snow cover pattern which is not consistent with the orographic features.

Quantile SND statistics in the period 1980-2005

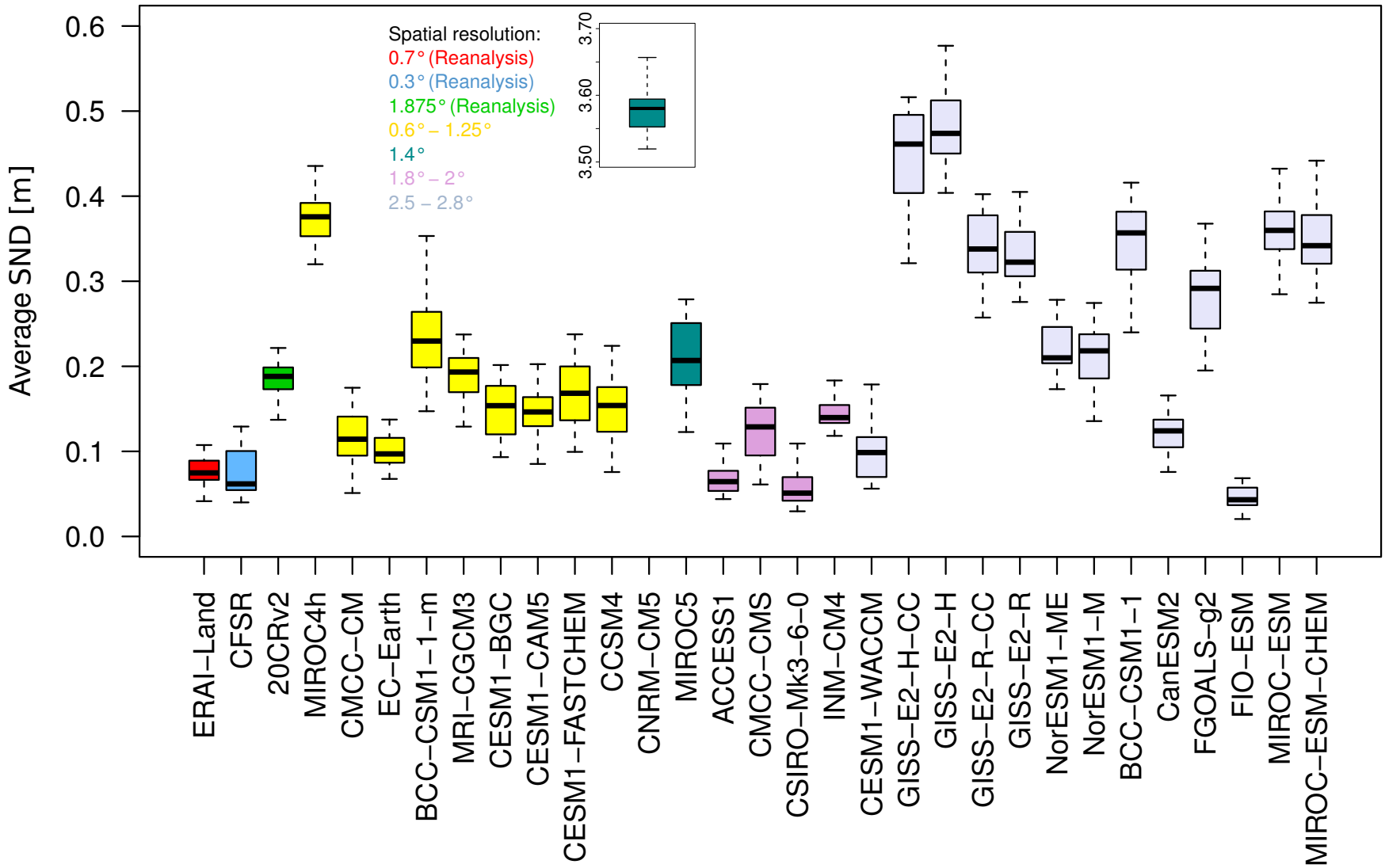

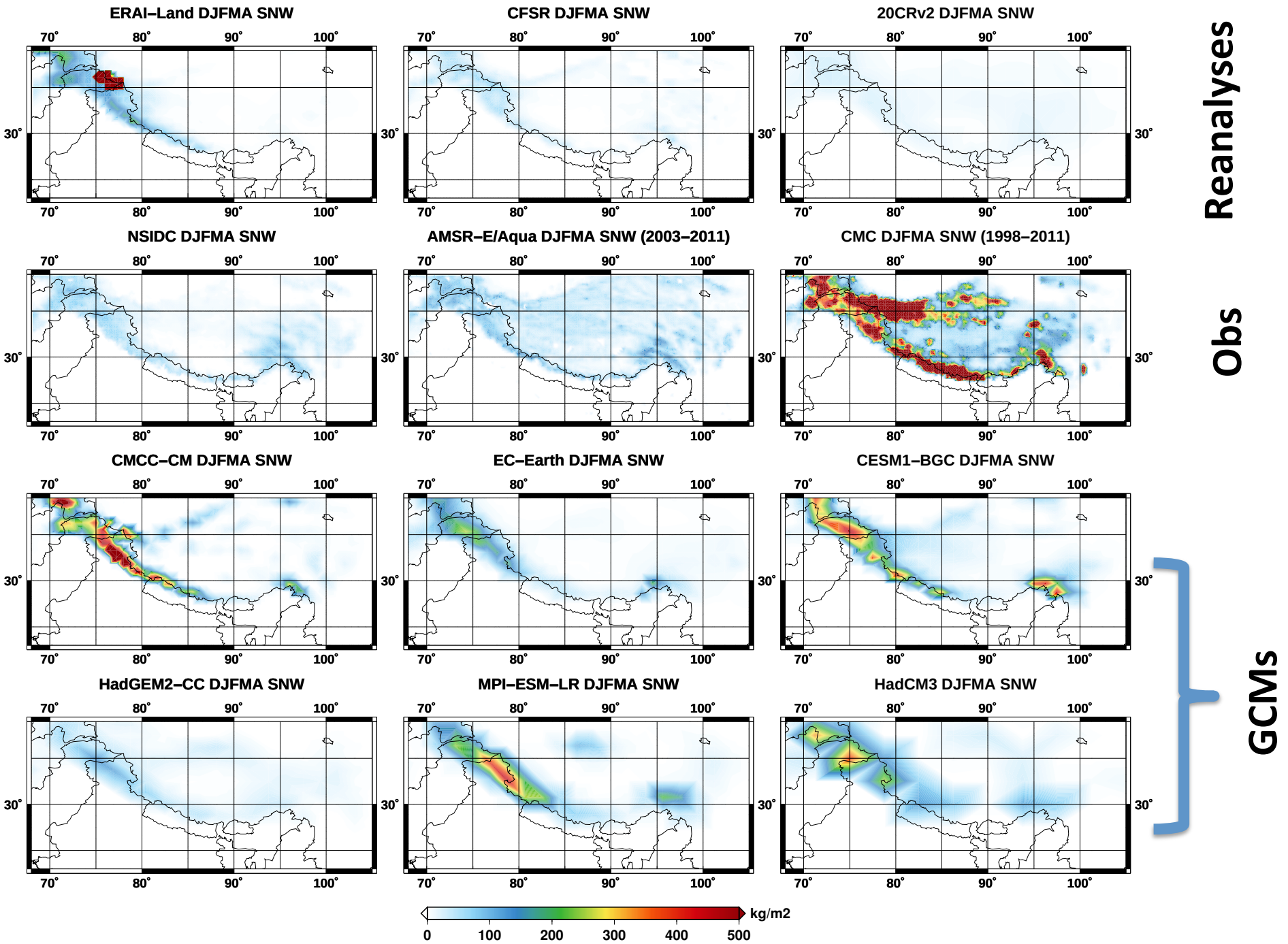
ERAI–Land DJFMA SNW
CFSR DJFMA SNW
20CRv2 DJFMA SNW
NSIDC DJFMA SNW
AMSR–E/Aqua DJFMA SNW (2003–2011)
CMC DJFMA SNW (1998–2011)
CMCC–CM DJFMA SNW
EC–Earth DJFMA SNW
CESM1–BGC DJFMA SNW
HadGEM2–CC DJFMA SNW
MPI–ESM–LR DJFMA SNW
HadCM3 DJFMA SNW
70˚
80˚
90˚
100˚
30˚
0
100
200
300
400
500
kg/m2
Reanalyses
Obs
GCMs

Quantile SWEstatistics in the period 1980-2005

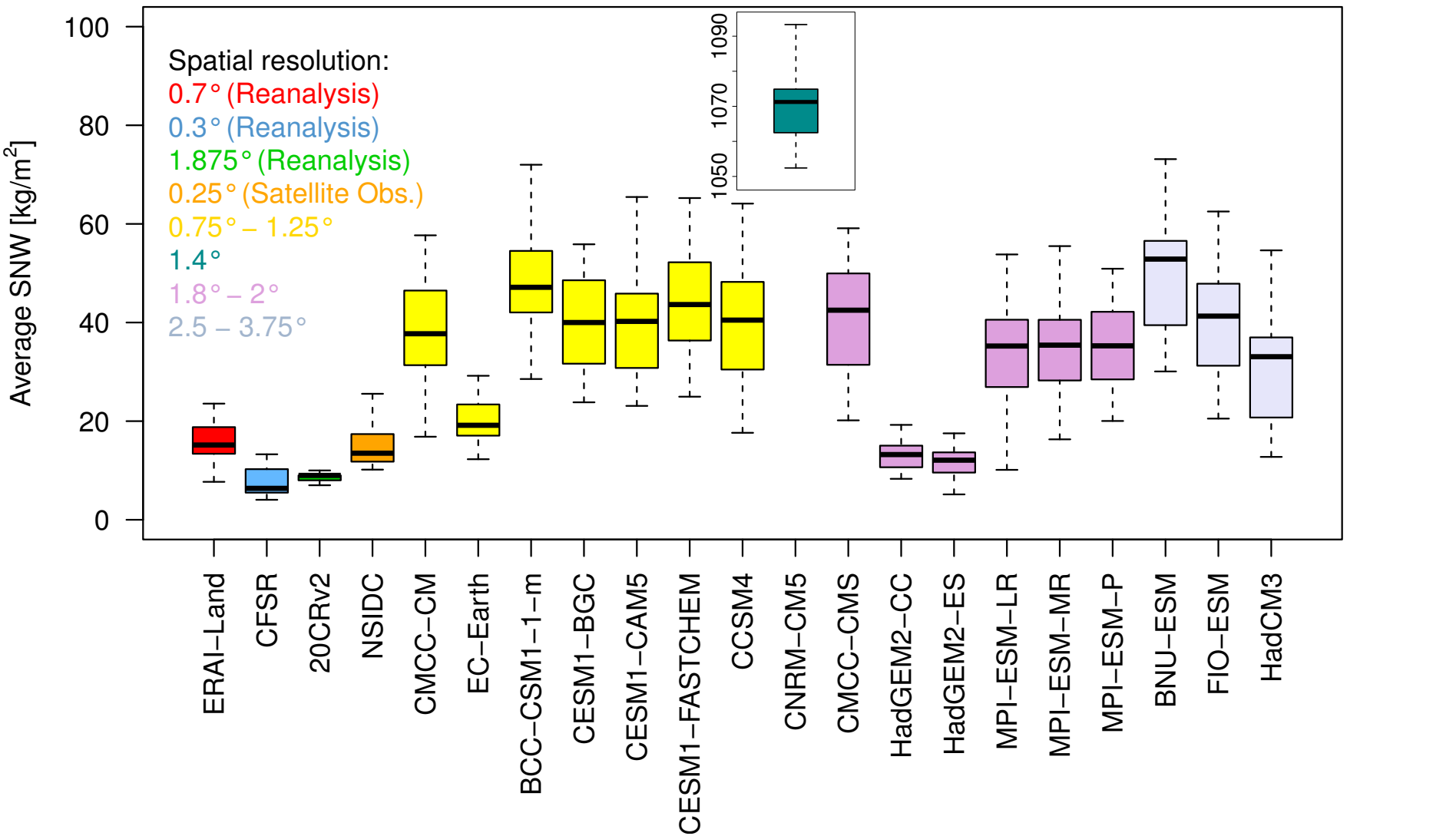

DJFMA snow depth projections – HKK above 1000 m a.s.l.

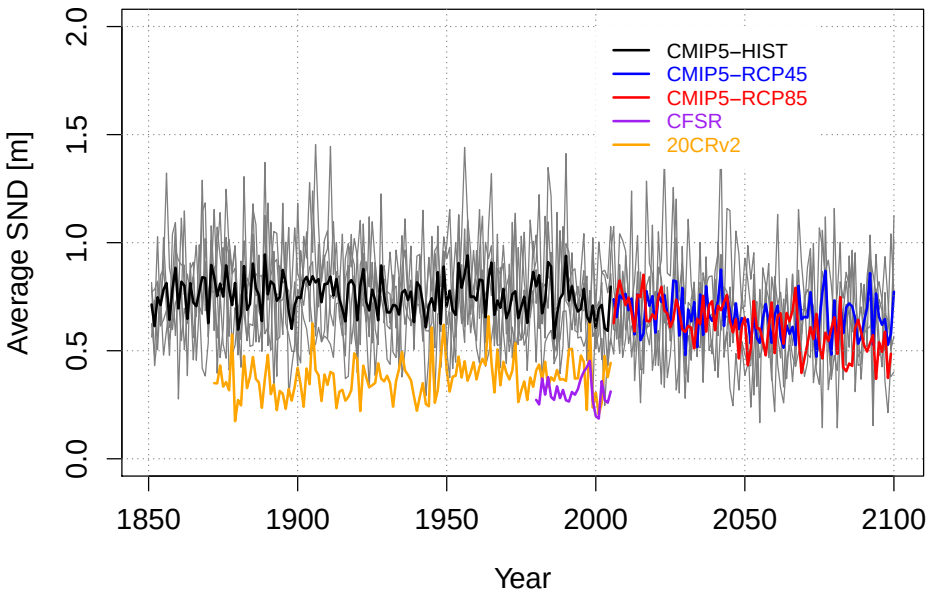

The HKK is expected to undergo a snow depth decrease of about **17%** **with respect to the historical mean value in the RCP4.5 scenario and of about 39% in the RCP8.5 scenario.**

DJFMA snow depth projections – Himalaya above 1000 m a.s.l.

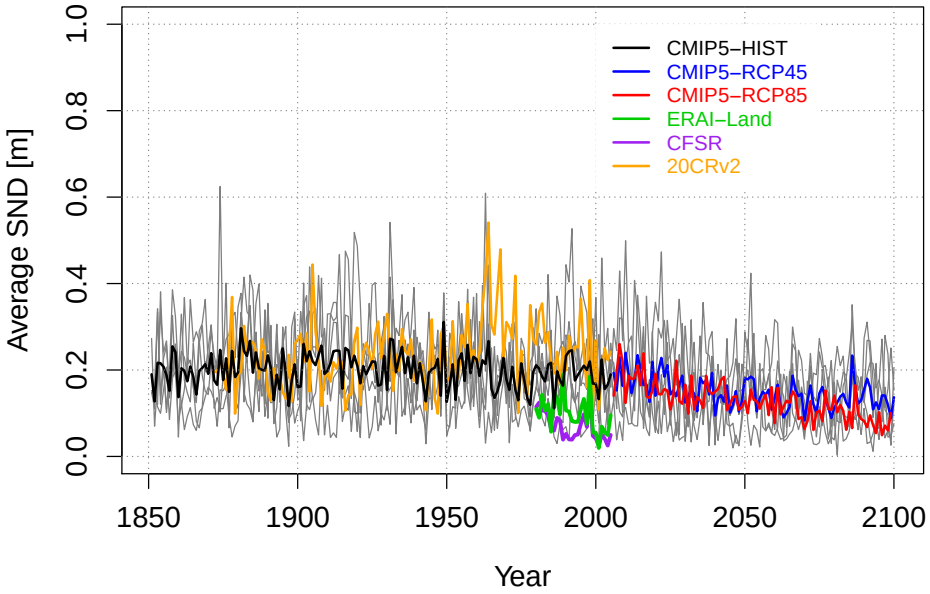

The Himalaya will face a significantly stronger decrease, ranging between 25% up to 50% of current conditions in the most extreme RCP8.5 scenario.

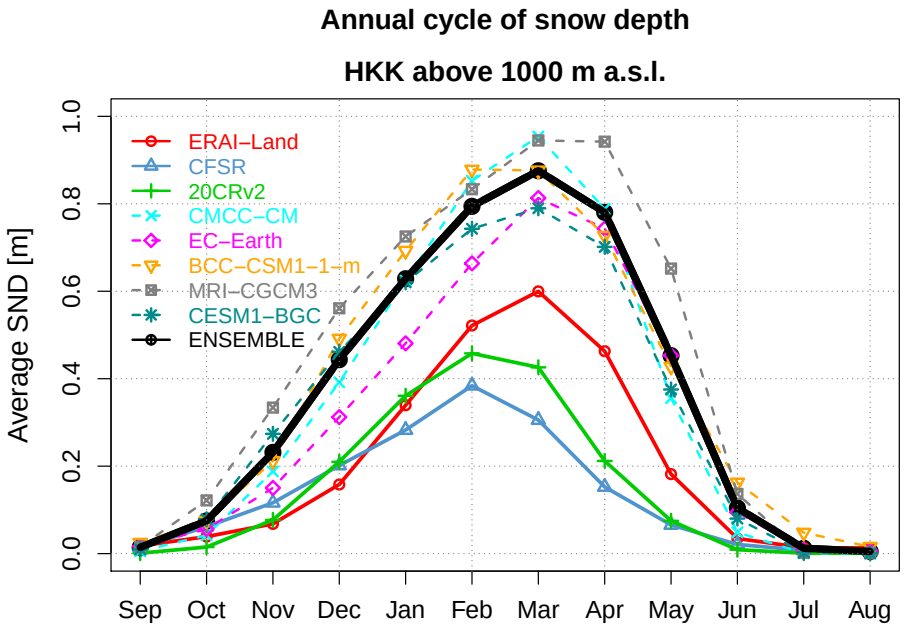
Annual cycle of snow depth
HKK above 1000 m a.s.l.
Average SND [m]
0.0
0.2
0.4
0.6
0.8
1.0
ERAI–Land
CFSR
20CRv2
CMCC–CM
EC–Earth
BCC–CSM1–1–m
MRI–CGCM3
CESM1–BGC
ENSEMBLE
Sep
Oct
Nov
Dec
Jan
Feb
Mar
Apr
May
Jun
Jul
Aug

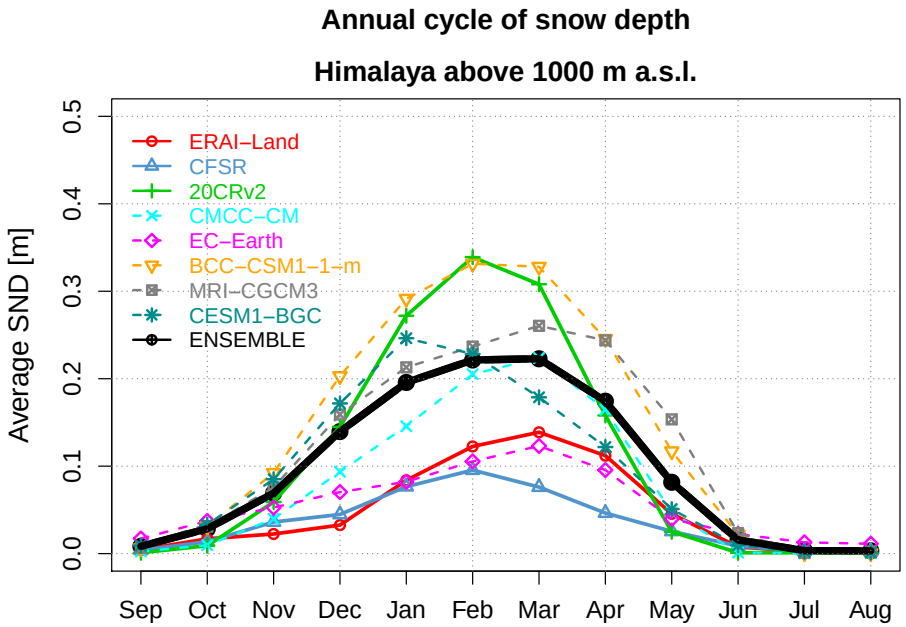
Annual cycle of snow depth
Himalaya above 1000 m a.s.l.
Average SND [m]
0.0
0.1
0.2
0.3
0.4
0.5
ERAI–Land
CFSR
20CRv2
CMCC–CM
EC–Earth
BCC–CSM1–1–m
MRI–CGCM3
CESM1–BGC
ENSEMBLE
Sep
Oct
Nov
Dec
Jan
Feb
Mar
Apr
May
Jun
Jul
Aug

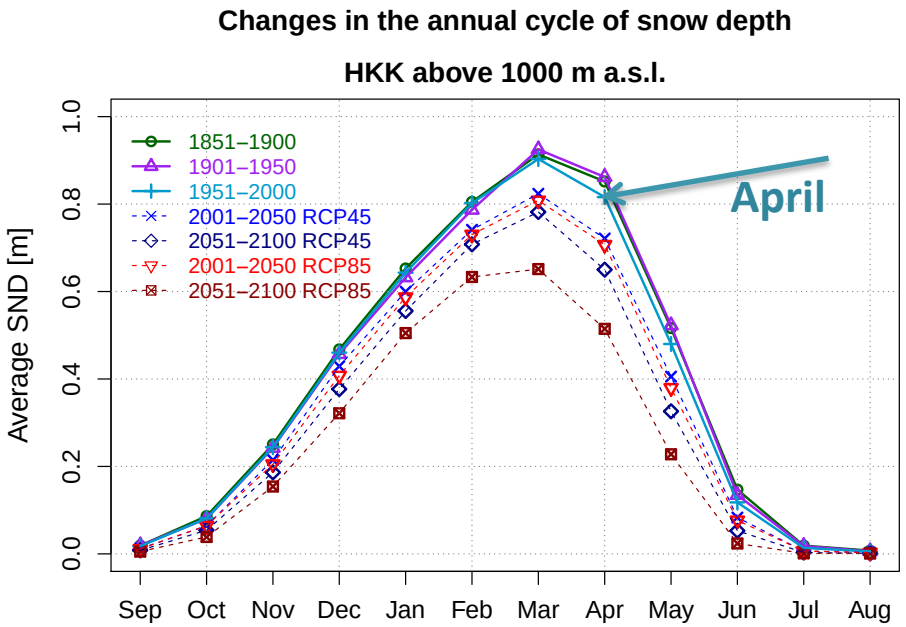
Changes in the annual cycle of snow depth
HKK above 1000 m a.s.l.
Average SND [m]
0.0
0.2
0.4
0.6
0.8
1.0
1851–1900
1901–1950
1951–2000
2001–2050 RCP45
2051–2100 RCP45
2001–2050 RCP85
2051–2100 RCP85
April
Sep
Oct
Nov
Dec
Jan
Feb
Mar
Apr
May
Jun
Jul
Aug

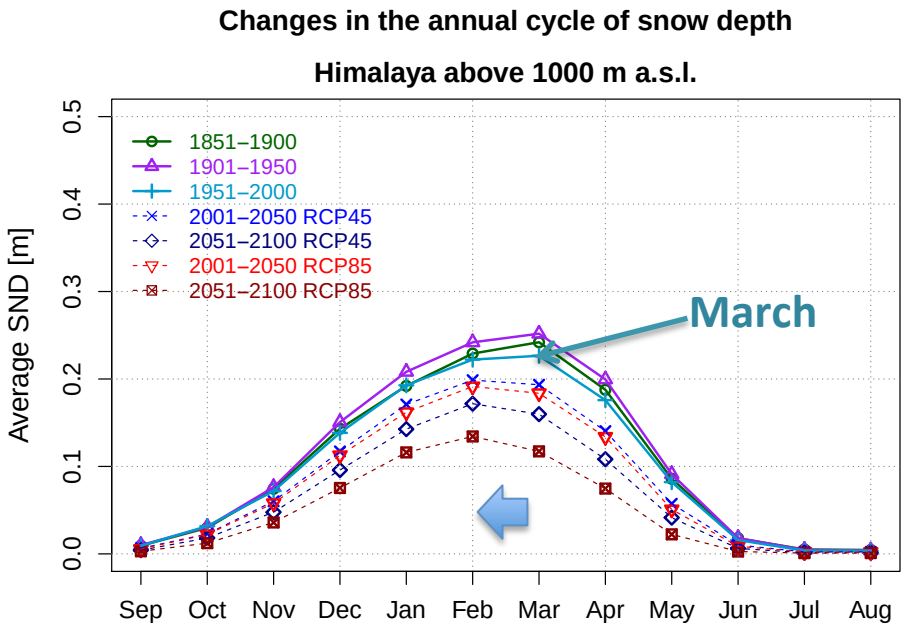
Changes in the annual cycle of snow depth
Himalaya above 1000 m a.s.l.
Average SND [m]
0.0
0.1
0.2
0.3
0.4
0.5
1851–1900
1901–1950
1951–2000
2001–2050 RCP45
2051–2100 RCP45
2001–2050 RCP85
2051–2100 RCP85
March
Sep
Oct
Nov
Dec
Jan
Feb
Mar
Apr
May
Jun
Jul
Aug

Simulation of snowpack dynamics in high elevation environments

Evaluation of the capability of different land-surface models in reproducing the snow dynamics in a high elevation site (Torgnon, 2160 m a.s.l., Western Italian Alps)

UTOPIA (SWE, SND)
CHTESSEL (SWE, SND)
AMUNDSEN (SWE)
GEOTOP (SWE, SND)

Forcing: station measurements at 30'.

Simulation of snowpack dynamics in high elevation environments

Evaluation of the capability of different land-surface models in reproducing the snow dynamics in a high elevation site (Torgnon, 2160 m a.s.l., Western Italian Alps)

UTOPIA (SWE, SND)
CHTESSEL (SWE, SND)
AMUNDSEN (SWE)
GEOTOP (SWE, SND)

Forcing: station measurements at 30'.

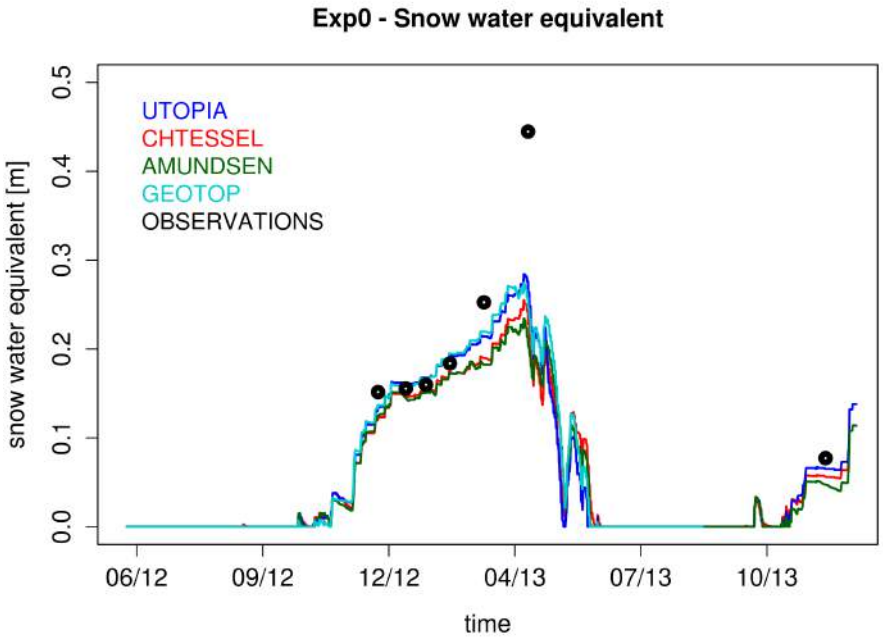

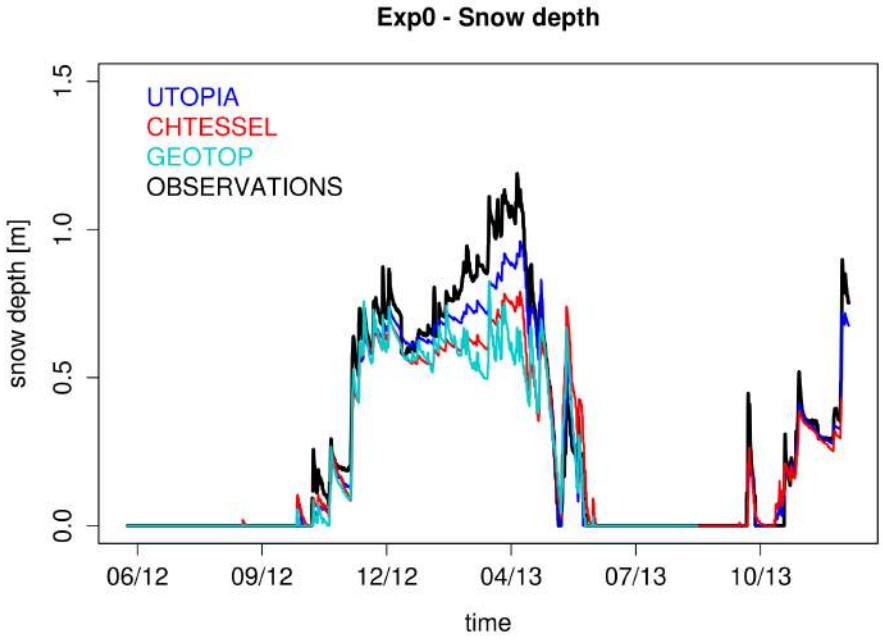

3. Simulations of the last 150 years climate with an Earth system models of intermediate complexity and preparation of paleoclimate simulations

The Planet Simulator (PlaSim)

- **Earth system Model of Intermediate Complexity** (Meteorological Institute, University of Hamburg)
- Suitable to run climate and **paleo-climate simulati**ons for time scales up to 10 thousand years, due to its medium complexity and associated less intensive computing requirements.
- **Components**:
  - Portable University Model of the Atmosphere (PUMA)
  - Ocean models (Mixed Layer or large-scale geostrophic ocean, LSG)
  - Land surface model (biosphere)
  - Sea ice

The Planet Simulator (PlaSim) – NEXTDATA

Climate response to CO2 forcing over the last ~150 years

Configurations:

- **T21 (~5.6°) and T42 (%2.8°)** horizontal resolutions
- **PUMA + ML; PUMA +LSG**
- **Perpetual simulations**: 1850 CO2 forcing (285 ppmv) and 2005 CO2 forcing(379 ppmv). 30 yrs with ML; 500 yrs with LSG.
- **Transient** simulations (forced by the historical CO2 concentrations from 1850 to 2005)
- **Variables:** Temperature and Precipitation (maps, time seres, zonal means)

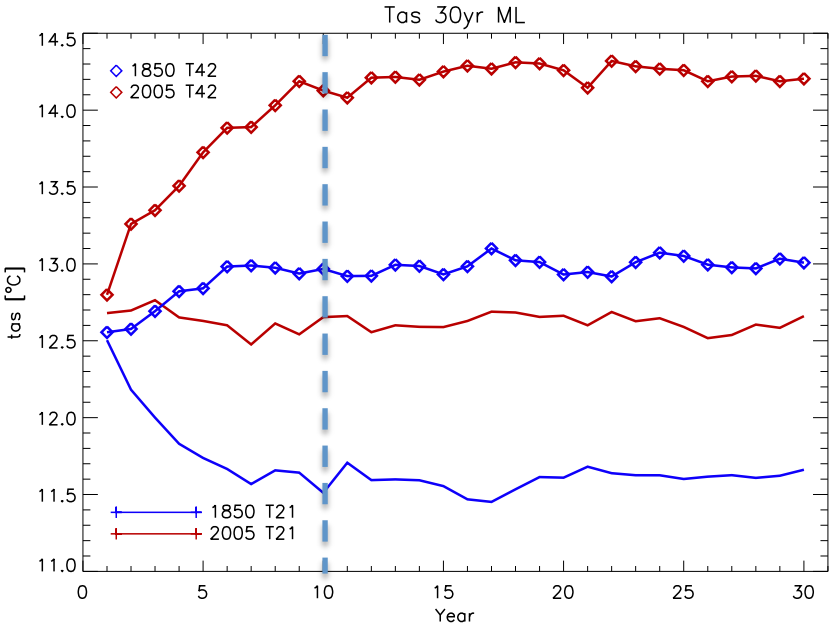

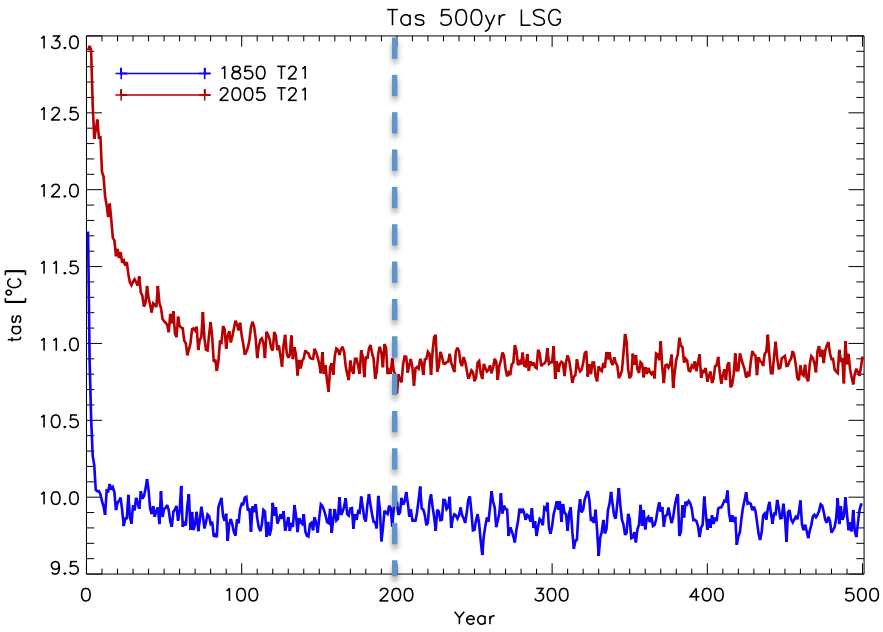

Perpetual Simulations - Temperature

PlaSim 2005 simulations

tas 2005 T21, ML

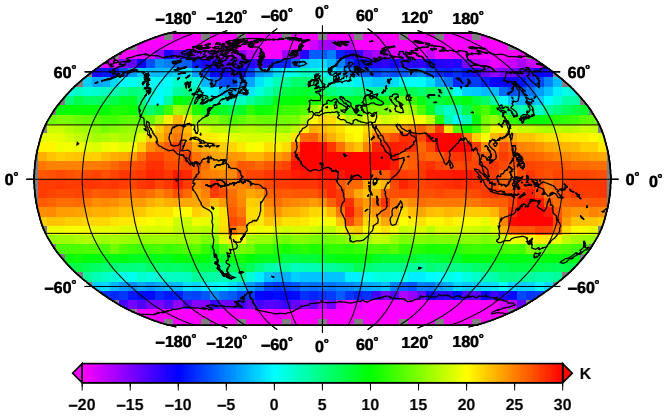

tas 2005 T42, ML

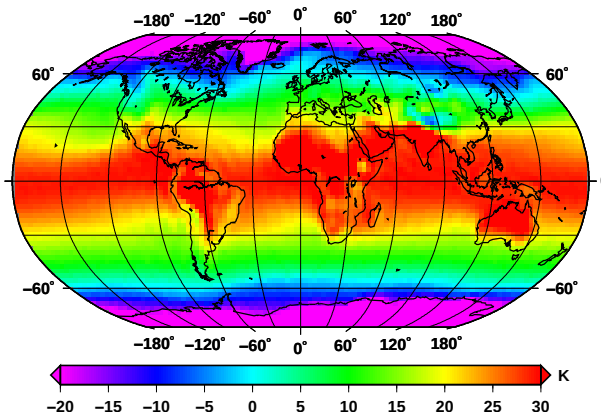

tas 2005 T21, ML+LSG

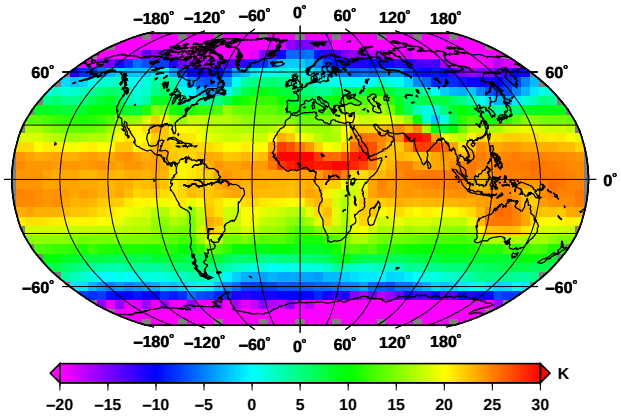

EC-Earth - PlaSim 2005

EC–Earth – Plasim 2005 T21, ML

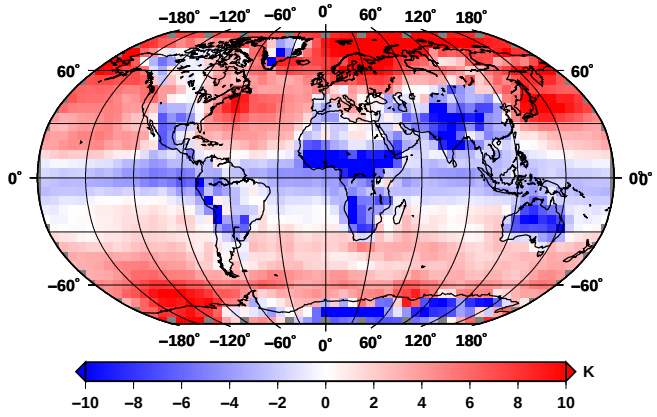

EC–Earth – Plasim 2005 T42, ML

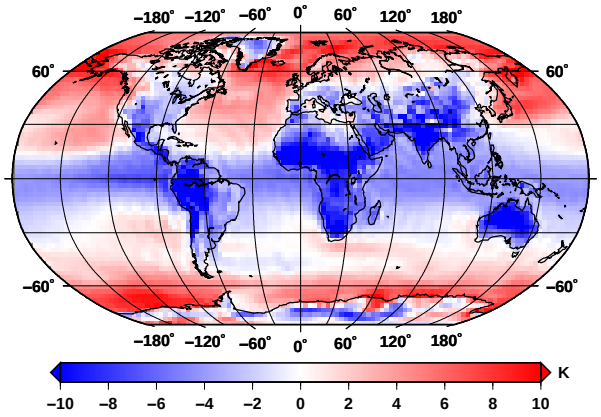

EC–Earth – Plasim 2005 T21, ML+LSG

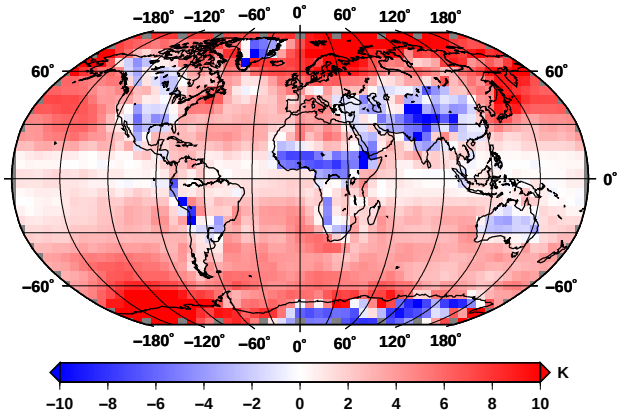

Perpetual Simulations - Precipitation

PlaSim 2005 simulations

pr 2005 T21, ML

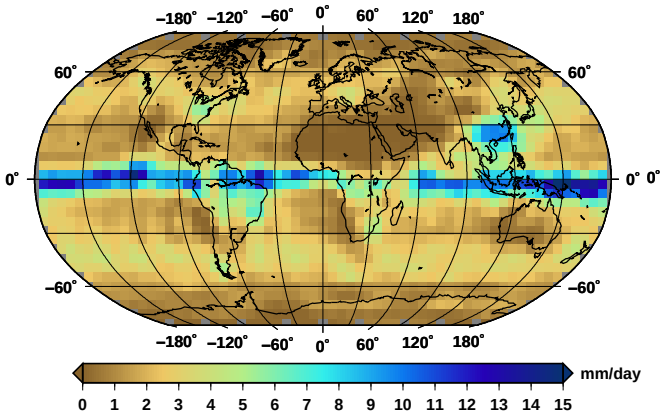

pr 2005 T42, ML

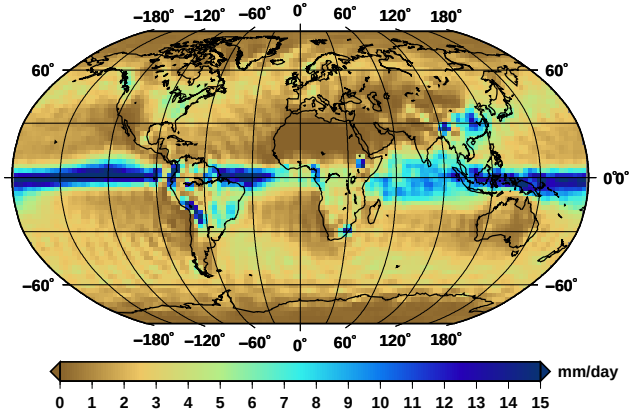

pr 2005 T21, LSG

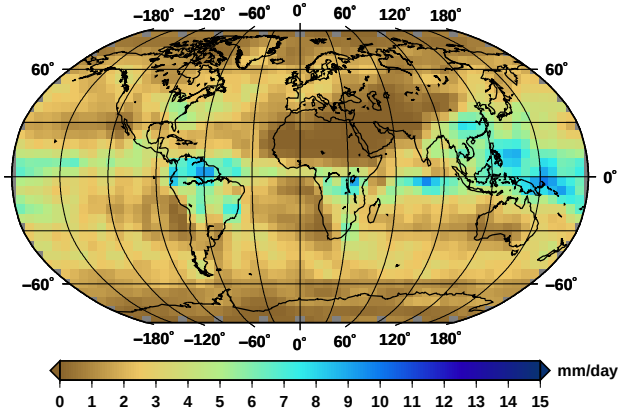

EC-Earth

pr 2005 T159 EC–Earth

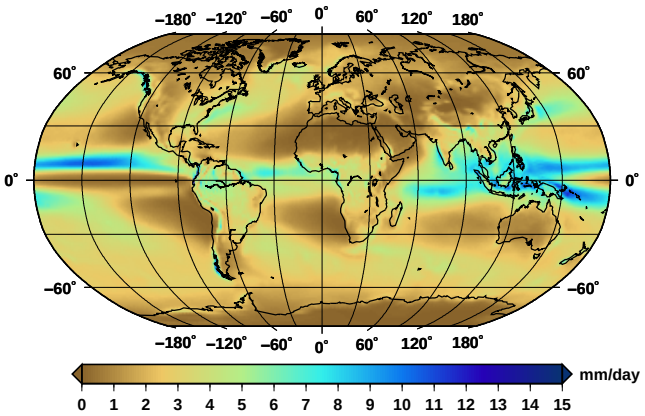

GPCP

GPCP Obs 2005

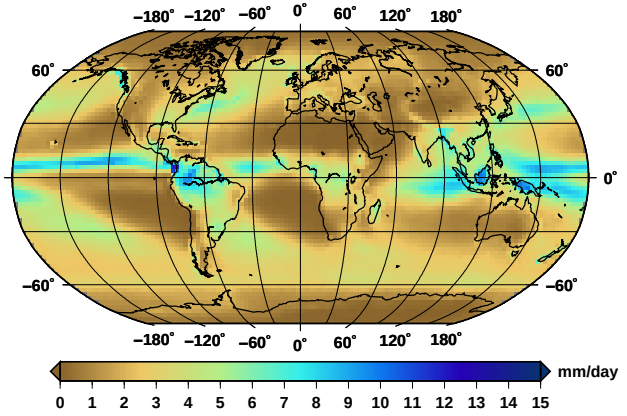

Perpetual Simulations - Precipitation

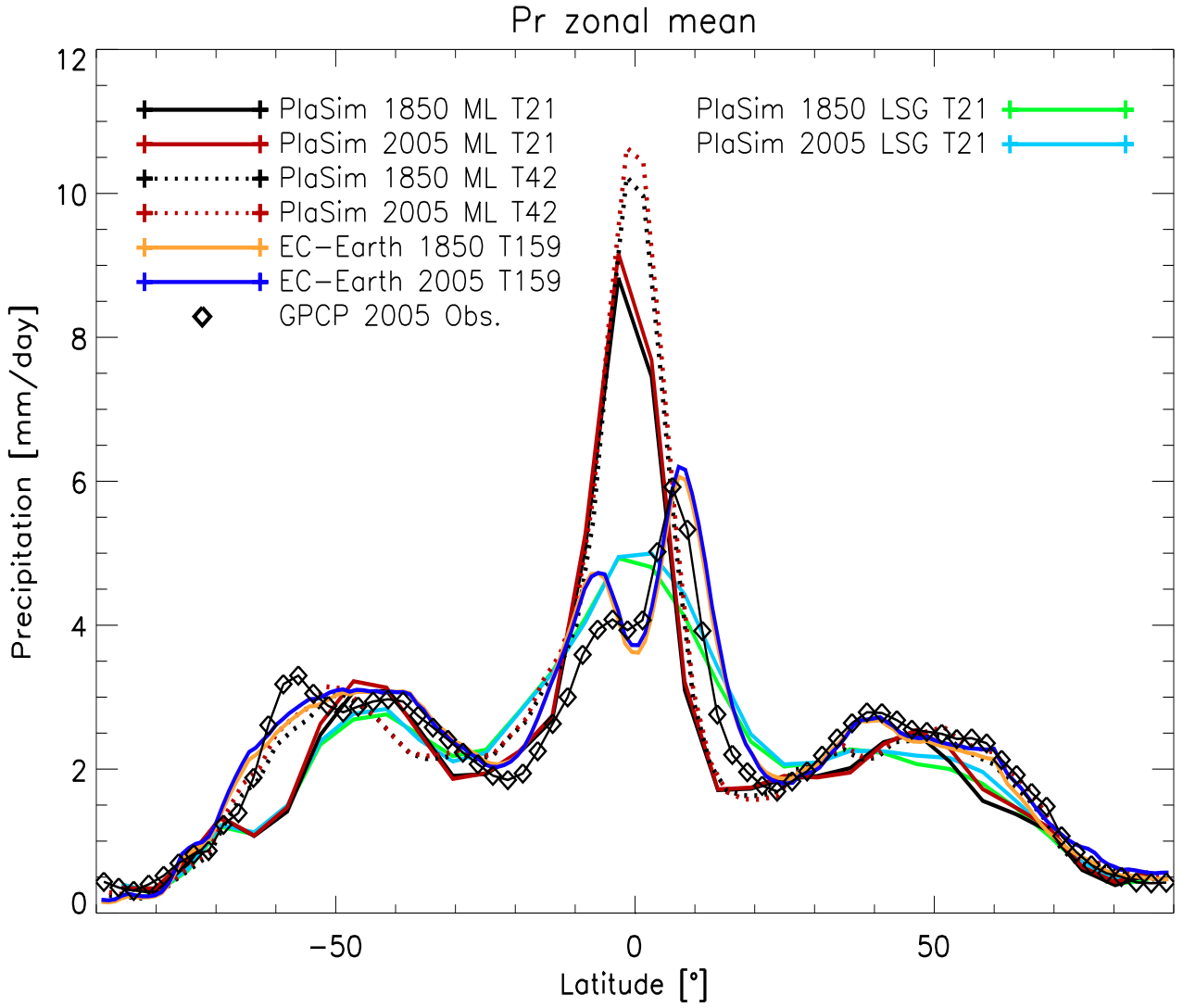

Transient Simulations - Temperature

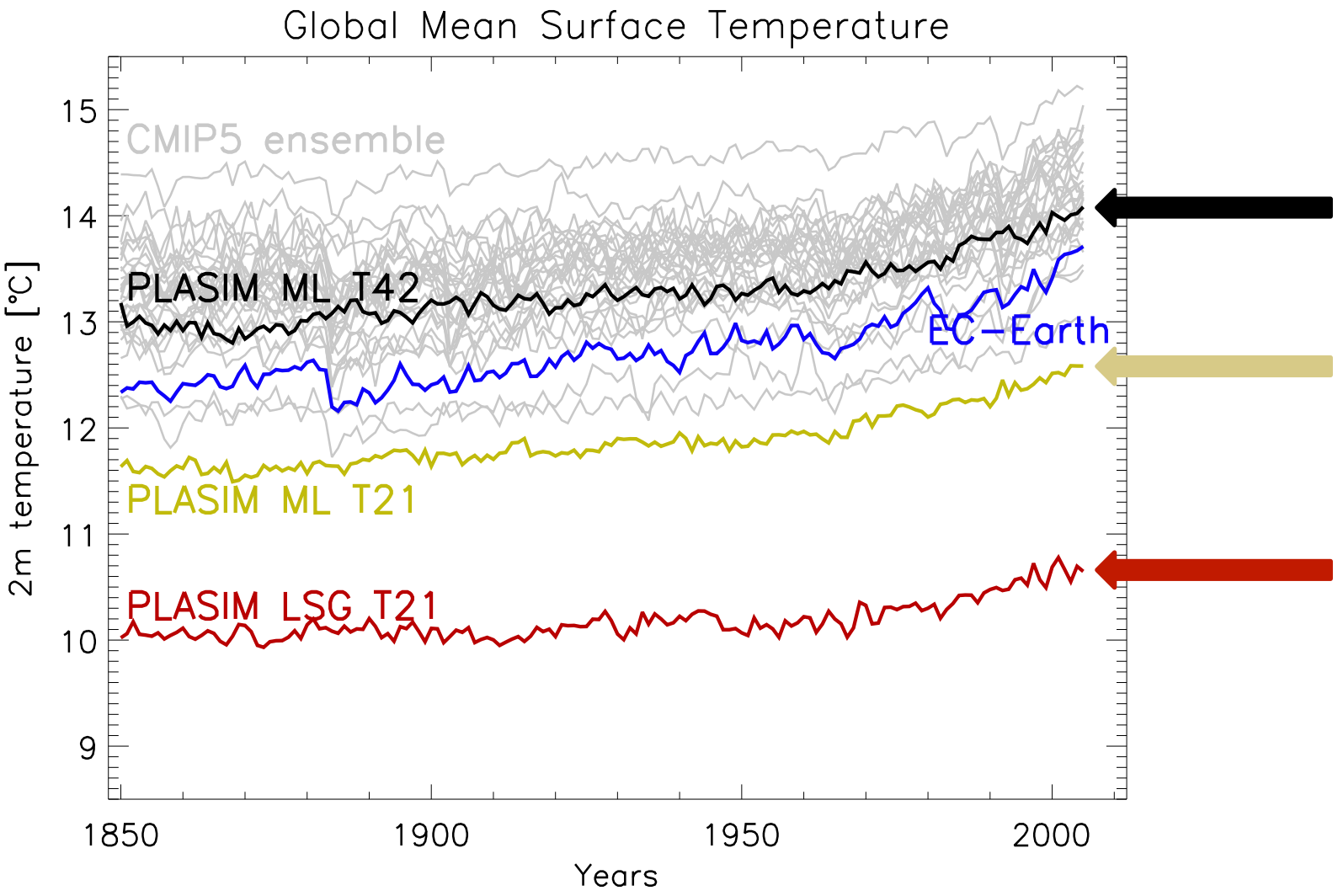

Annual cycle Climatology in the HKK sub-region

Time vs latitude Hovmöller plots of the zonal mean monthly precipitation

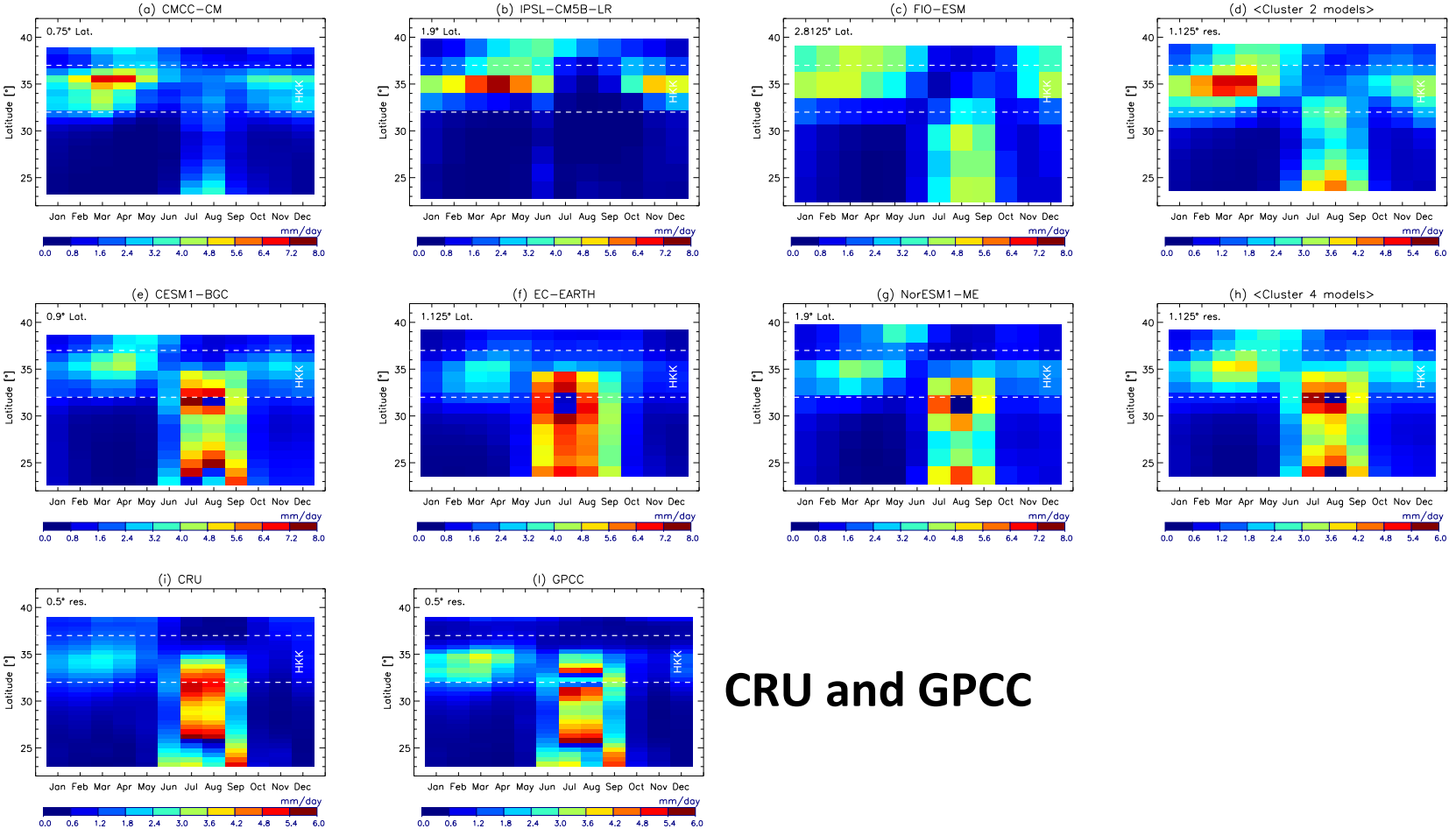

Cluster 2 (KO)

Cluster 4 (OK)

CRU and GPCC

Palazzi, von Hardenberg, Terzago and Provenzale, under revision, Clim Dyn

The possible role of ENSO in weakening the NAO-precipitation correlation

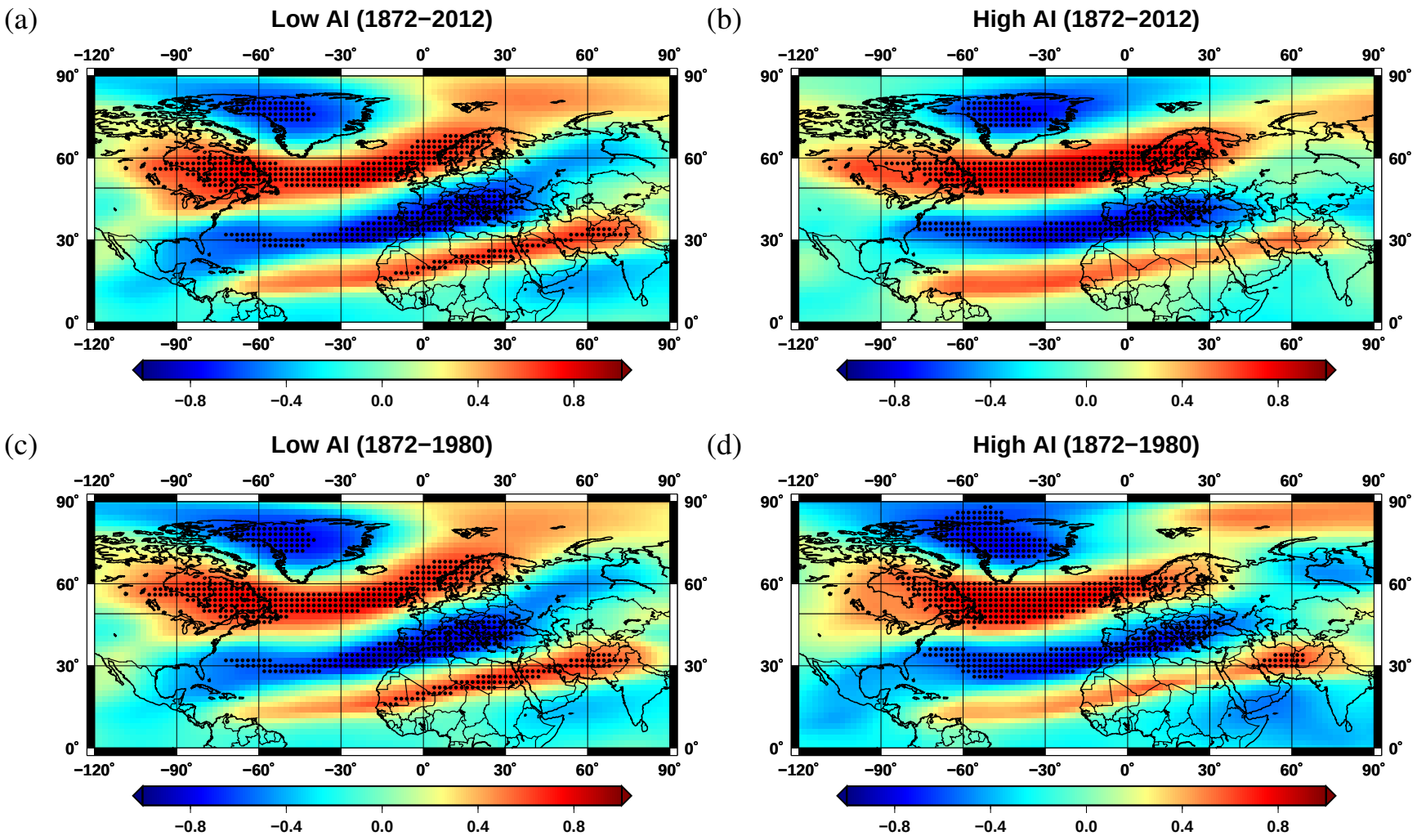

Composites of the correlation fields between the NAOI and 250 hPa zonal wind corresponding to (a,c) low and (b,d) high AI values. Correlation fields are computed on 21-year windows.